The Abdus Salam
International Centre for Theoretical Physics

United Nations
Educational, Scientific and
Cultural Organization

IAEA
International Atomic Energy Agency

1856-66

2007 Summer College on Plasma Physics

30 July - 24 August, 2007

Localized envelope excitations in pair plasmas

I. Kourakis
Ruhr Univers. Bochum, Germany

INSTITUTE OF PHYSICS PUBLISHING JOURNAL OF PHYSICS A: MATHEMATICAL AND GENERAL

J. Phys. A: Math. Gen. **39** (2006) 13817–13830 doi:10.1088/0305-4470/39/44/014

Electrostatic mode envelope excitations in e–p–i plasmas—application in warm pair ion plasmas with a small fraction of stationary ions

A Esfandyari-Kalejahi[1], I Kourakis[2,3], M Mehdipoor[1] and P K Shukla[3]

[1] Department of Physics, Faculty of Science, Azarbaijan University of Tarbiat Moallem, 51745-406 Tabriz, Iran
[2] Universiteit Gent, Sterrenkundig Observatorium, Krijgslaan 281, B-9000 Gent, Belgium
[3] Fakultät für Physik und Astronomie, Institut fürTheoretische Physik IV, Ruhr-Universität Bochum, D-44780 Bochum, Germany

E-mail: ra-esfandyari@azaruniv.edu, ioannis@tp4.rub.de and ps@tp4.rub.de

Received 13 May 2006, in final form 6 September 2006
Published 17 October 2006
Online at stacks.iop.org/JPhysA/39/13817

Abstract

The nonlinear propagation of amplitude-modulated electrostatic wavepackets in an electron–positron–ion (e–p–i) plasma is considered, by employing a two-fluid plasma model. Considering propagation parallel to the external magnetic field, two distinct electrostatic modes are obtained, namely a quasi-thermal acoustic-like lower mode and a Langmuir-like optic-type upper one. These results equally apply in warm pair ion (e.g. fullerene) plasmas contaminated by a small fraction of stationary ions (or dust), in agreement with experimental observations and theoretical predictions in pair plasmas. Considering small yet weakly nonlinear deviations from equilibrium, and adopting a multiple-scales perturbation technique, the basic set of model equations is reduced to a nonlinear Schrödinger (NLS) equation for the slowly varying electric field perturbation amplitude. The analysis reveals that the lower (acoustic) mode is mostly stable for large wavelengths, and may propagate in the form of a dark-type envelope soliton (a void) modulating a carrier wavepacket, while the upper linear mode is intrinsically unstable, and thus favours the formation of bright-type envelope soliton (pulse) modulated wavepackets. The stability (instability) range for the acoustic (Langmuir-like optic) mode shifts to larger wavenumbers as the positive-to-negative ion temperature (density) ratio increases. These results may be of relevance in astrophysical contexts, where e–p–i plasmas are encountered, and may also serve as prediction of the behaviour of doped (or dust-contaminated) fullerene plasmas, in the laboratory.

PACS numbers: 52.30.Ex, 52.27.Ep, 52.35.Fp, 52.35.Mw

1. Introduction

A great deal of research effort has recently been devoted to pair plasmas, i.e. large ensembles of charged matter consisting of equal mass and opposite charge sign particles. In contrast to ordinary (electron–ion, e–i) plasmas, where the large mass difference between particle species imposes distinct frequency scales, the positively and negatively charged particles in pair plasmas respond on the same scale. Nevertheless, the characteristics of waves cannot always be deduced from what is obtained from e–i plasmas by simply letting particle masses to be equal to one-another. For instance, it is known that parallel propagating linear electromagnetic waves are not circularly but linearly polarized in pair plasmas, and Faraday rotation is absent in this case [1]. Furthermore, ion-acoustic waves have no counterpart in electron–positron (e–p) plasmas, where the electrostatic wave dispersion is of high frequency Langmuir type [2, 3]. The properties of e–p plasmas have been investigated by several authors [4–7]. Recently, the production of pair fullerene-ion plasmas in laboratory [8–10] has enabled experimental studies of pair plasmas rid of intrinsic problems involved in electron–positron plasmas, namely pair recombination processes and strong Landau damping.

In real, e.g. astrophysical contexts, e–p plasmas are also characterized by the presence of positive ions, in addition to electrons and positrons. Electron–positron–ion (e–p–i) plasmas appear in the early universe [11], active galactic nuclei [12] and in pulsar magnetospheres [13]. Furthermore, e–p–i plasmas can be created in laboratory plasmas [14–17]. The standard description of e–p–i plasmas adopted here considers fully ionized plasmas which consist of two populations of different charge signs possessing equal masses and absolute charge values ($m_1 = m_2 = m_e$, $q_1 = -q_2 = +e$), in addition to a population of positively charged ions ($m_3 = M$, $q_3 = +Z_3 e$); see for instance [18–22]. On the other hand, one may anticipate the injection of a small fraction of charged massive particles (an ion species, or dust particulates) into fullerene pair-ion plasma [8–10] (doping) in order to produce three-component plasmas which may accommodate new physical phenomena.

As far as electrostatic (ES) plasma modes [23, 24] are concerned, the occurrence and properties of nonlinear ES waves in e–p–i *plasmas* have been investigated by several authors. From a theoretical point of view, e–p–i plasmas are characterized by new, modified properties and conditions for the existence of arbitrary amplitude localized ES nonlinear excitations (which are typically modelled via the Sagdeev pseudopotential formalism [25–28]). Furthermore, small amplitude-modulated wavepackets, generically related to nonlinear Schrödinger theories [29], may be investigated via a (Krylov–Bogoliubov–Mitropolsky) reductive perturbation technique [30–32]. The nonlinear modulation of such ion-acoustic ES wavepackets was indeed studied by Salahuddin *et al* [33] in e–p–i plasmas, by considering (low-frequency) ion-acoustic oscillations against a Maxwellian background of thermalized electrons and positrons. Here, we aim at investigating the opposite edge of the ES frequency range, namely high-frequency oscillations of (light mass) electrons and positrons (or pair ions) against a neutralizing background of (heavier) ions which, given the frequency range of interest, may be considered to be immobile. A similar study with respect to pure (two-component) pair plasmas was carried out in [34, 35].

The present study is devoted to an investigation of the nonlinear amplitude modulation of electrostatic modes propagating parallel to the external magnetic field, in e–p–i plasmas. The model readily applies in pair-ion (e.g. fullerene) plasmas contaminated by a small fraction of uniform and stationary (heavier) positive ions (or, say, dust particulates). The two electron and positron (or pair ion) fluids are assumed to be warm and have a similar (yet not necessarily equal) temperature, while the neutralizing background ions are stationary. Positive background ions are implicitly considered here, although the formalism may also apply for negative ions

(e.g. dust particles) as well. Relying on a two-fluid plasma description and adopting a slowly varying amplitude hypothesis, we shall employ a multiple-scale technique [30–32] in order to derive a nonlinear Schrödinger-(NLS) type evolution equation [29] for the amplitude of weakly nonlinear electrostatic perturbations from equilibrium. The amplitude's (modulational) stability will then be studied, and the occurrence of modulated envelope excitations will be discussed. Also, the influence of the value of positron-to-electron (or positive-to-negative particle) density and temperature ratios on the modulational stability profile of ES waves will be elucidated.

The layout of this paper is as follows. In section 2, the analytical model is introduced and then employed, in section 3, as the basis of a perturbative analysis, by introducing appropriate slow space and time evolution scales. An NLS-type equation is derived, governing the (slow) amplitude evolution in time and space. The stability analysis and associated expressions for envelope soliton solutions of the NLSE are outlined in section 4. Section 5 is devoted to a discussion of the linear stability of ES waves by means of a numerical investigation of relevant quantities (NLSE coefficients). Finally, our conclusions are summarized in section 6.

2. The model equations

We shall consider a three-component plasma consisting of two inertial species, say 1 and 2, which have equal masses and equal absolute charges of the opposite sign, i.e. $q_1 = -q_2 = +Ze$, $m_1 = m_2 = m$ and a third species, say 3, having a constant density n_3, particle mass $m_3 \neq m$ and particle charge $Z_3 e \neq Ze$. In specific, this picture applies to e–p–i plasmas, for $Z = 1$, or in pair-ion (e.g. fullerene) [8–10], for $Z = 1$, 'doped' by the injection of a third charged particle species of higher mass.

The two-fluid plasma-dynamical (moment) equations for our three-component plasma include the two density (continuity) equations

$$\frac{\partial n_\alpha}{\partial t} + \vec{\nabla} \cdot (n_\alpha \vec{U}_\alpha) = 0, \tag{1}$$

and the two momentum equations

$$\frac{\partial \vec{U}_\alpha}{\partial t} + (\vec{U}_\alpha \cdot \vec{\nabla})\vec{U}_\alpha = -\frac{q_\alpha}{m_\alpha}\vec{\nabla}\phi - \frac{\vec{\nabla} p_\alpha}{m_\alpha n_\alpha}, \tag{2}$$

where the subscript α denotes either species 1 (i.e. the positive ions, or positrons) for $\alpha = +$, or species 2 (i.e. the negative ions, or electrons) for $\alpha = -$. The moment variables n_α, $\vec{U}_\alpha$ and p_α denote the density, fluid velocity and pressure of species α, respectively. The Lorentz force term is neglected, since wave propagation parallel to external magnetic field is assumed. The electric field is provided by the electric potential φ, which obeys Poisson's equation:

$$\nabla^2 \varphi = 4\pi e Z(n_- - n_+) - 4\pi Z_3 e n_3. \tag{3}$$

The background ion density n_3 is constant. The right-hand side on equation (3) is assumed to cancel at equilibrium, due to the quasi-neutrality condition $Z(n_{-,0} - n_{+,0}) - Z_3 n_3 = 0$. The system of equations (1) to (3) is closed by assuming an explicit density dependence of the pressure in the form $p_\alpha = C n_\alpha^\gamma$, where γ is the ratio of specific heats. Combining this assumption with the equation of state (at equilibrium) $p_{\alpha,0} = n_{\alpha,0} k_B T_\alpha$ (where T_α denotes the temperature of species α; k_B is Bolztmann's constant), the pressure term may be rearranged as $\vec{\nabla} p_\alpha / n_\alpha = \gamma K_B T_\alpha n_{\alpha 0}^{1-\gamma} n_\alpha^{\gamma-2} \vec{\nabla} n_\alpha$.

The model equations may be cast into a reduced (dimensionless) form by scaling the time and space variables as $t' \equiv \omega_{p,-} t$ and $x' \equiv x/\lambda_{D,-}$, respectively. We have defined the plasma

frequency $\omega_{p,\alpha} = \left(4\pi n_0 q_\alpha^2/m\right)^{1/2}$ (see that $\omega_{p,-} = \omega_{p,+} = \omega_p$ if $n_{+,0} = n_{-,0}$, only) and the Debye length $\lambda_{D,\alpha} = \left(K_B T_\alpha/m\,\omega_{p,\alpha}^2\right)^{1/2}$ (for $\alpha = +, -$). The density, velocity and electric potential state variables are scaled as $n'_\alpha = n_\alpha/n_{-,0}$, $u'_\alpha = u_\alpha/c_s$ and $\varphi' = \varphi/\varphi_0$, respectively, where we have defined the characteristic (sound) speed $c_s = (k_B T_-/m)^{1/2}$ (for negative ions) and the characteristic potential scale $\varphi_0 = K_B T_-/Ze$ (the primes will be dropped for simplicity). Combining these definitions and considering a one-dimensional geometry (along x), the model equations reduce to

$$\frac{\partial n_\alpha}{\partial t} + \vec{\nabla}\cdot(n_\alpha \vec{U}_\alpha) = 0, \tag{4}$$

$$\frac{\partial \vec{U}_\alpha}{\partial t} + (\vec{U}_\alpha\cdot\vec{\nabla})\vec{U}_\alpha = -\alpha\vec{\nabla}\phi - \frac{\gamma T_\alpha}{T_-} n_\alpha^{\gamma-2}\vec{\nabla} n_\alpha, \tag{5}$$

and

$$\nabla^2\varphi = (n_- - n_+) - \frac{Z_3}{Z} n_3, \tag{6}$$

where $\alpha = +, -$ is used as a subscript (denoting species) *and* as a factor ($= \pm 1$), throughout this text. In equilibrium, the neutrality condition $1 - \beta - \delta(Z_3/Z) = 0$ holds. Here we have defined the parameters $\beta = n_{+0}/n_{-0}$ and $\delta = n_3/n_{-0}$. See that positively charged background ions will be implicitly considered here ($Z_3 > 0$, i.e. $\delta > 0$), although the formalism readily applies for negatively charged massive particles (e.g. dust), for $Z_3 < 0$, i.e. $\delta > 0$. We note that $\beta < 1$ for $\delta \neq 0$ (in the former case, considered in the following; the opposite holds in the negative-ion case); the case $\delta = 0$ refers to 'pure' pair plasma. The choice $\gamma = 3$ is made in the following, accounting for one-dimensional wave propagation.

3. Methodology—derivation of an amplitude evolution equation

3.1. The perturbative analysis

In order to obtain an explicit evolution equation describing the propagation of modulated EA envelopes, from the model equations (4)–(6), we shall employ the standard reductive perturbation (multiple scales) technique [30–32]. The independent variables x and t are stretched as $\xi = \varepsilon(x - \lambda t)$ and $\tau = \varepsilon^2 t$, where ε is a small (real) parameter; here, λ is a free (real) parameter, which is to be later determined as the wave's group velocity by compatibility requirements. The dependent variables are expanded as

$$n_- = 1 + \sum_{n=1}^{\infty}\sum_{l=-\infty}^{+\infty} \varepsilon^n n_{-,l}^{(n)}(\xi,\tau)\,\mathrm{e}^{\mathrm{i}l(kx-\omega t)}, \qquad n_+ = \beta + \sum_{n=1}^{\infty}\sum_{l=-\infty}^{\infty} \varepsilon^n n_{+,l}^{(n)}(\xi,\tau)\,\mathrm{e}^{\mathrm{i}l(kx-\omega t)}$$

$$U_+ = \sum_{n=1}^{\infty}\sum_{l=-\infty}^{\infty} \varepsilon^n U_{+,l}^{(n)}(\xi,\tau)\,\mathrm{e}^{\mathrm{i}l(kx-\omega t)}, \qquad U_- = \sum_{n=1}^{\infty}\sum_{l=-\infty}^{\infty} \varepsilon^n U_{-,l}^{(n)}(\xi,\tau)\,\mathrm{e}^{\mathrm{i}l(kx-\omega t)} \tag{7}$$

$$\phi = \sum_{n=1}^{\infty}\sum_{l=-\infty}^{\infty} \varepsilon^n \phi_l^{(n)}(\xi,\tau)\,\mathrm{e}^{\mathrm{i}l(kx-\omega t)}$$

where ω and k are the real parameters denoting the wave's frequency and wavenumber; the reality condition $A_{-l}^{(n)} = A_l^{(n)*}$ is met by all state variables; the star superscript denotes the complex conjugate of the (complex) harmonic amplitudes.

Substituting the expansion ansatz (7) and the stretched variables ξ, τ into equations (4)–(6), and then isolating distinct orders in ε, we obtain the nth order reduced density equation

$$-\lambda\frac{\partial n_{\alpha,l}^{(n-1)}}{\partial\xi}+\frac{\partial n_{\alpha,l}^{(n-2)}}{\partial\tau}-\mathrm{i}l\omega n_{\alpha,l}^{(n)}+\mathrm{i}lk\kappa_\alpha U_{\alpha,l}^{(n)}+\kappa_\alpha\frac{\partial U_{\alpha,l}^{(n-1)}}{\partial\xi}$$
$$+\sum_{n'=1}^{\infty}\sum_{l'=-\infty}^{\infty}\left[\mathrm{i}lkn_{\alpha,l'}^{(n')}U_{\alpha,l-l'}^{(n-n')}+\frac{\partial}{\partial\xi}\left(n_{\alpha l'}^{(n')}U_{\alpha,l-l'}^{(n-n'-1)}\right)\right]=0, \tag{8}$$

density equation

$$\frac{\partial U_{\alpha,l}^{(n-2)}}{\partial\tau}-\lambda\frac{\partial U_{\alpha,l}^{(n-1)}}{\partial\xi}-\mathrm{i}l\omega n_{\alpha,l}^{(n)}+\sum_{n'=1}^{\infty}\sum_{l'=-\infty}^{\infty}\left[\mathrm{i}l'kU_{\alpha,l-l'}^{(n-n')}U_{-,l}^{(n)}+U_{\alpha,l-l'}^{(n-n'-1)}\frac{\partial U_{\alpha,l'}^{(n')}}{\partial\xi}\right]$$
$$=-\alpha\frac{\partial\varphi_l^{(n-1)}}{\partial\xi}-\mathrm{i}l\alpha k\varphi_l^{(n)}-3\mathrm{i}lk\kappa_\alpha n_{\alpha,l}^{(n)}-3\kappa_\alpha\sigma_\alpha\frac{\partial n_{\alpha,l}^{(n-1)}}{\partial\xi}$$
$$-3\sum_{n'=1}^{\infty}\sum_{l'=-\infty}^{\infty}\left[\mathrm{i}l'n_{\alpha,l-l'}^{(n-n')}kn_{-,l'}^{(n')}+n_{\alpha,l-l'}^{(n-n'-1)}\frac{\partial n_{\alpha,l'}^{(n')}}{\partial\xi}\right], \tag{9}$$

and Poisson's equation

$$\frac{\partial^2\varphi_l^{(n-2)}}{\partial\xi^2}-l^2k^2\varphi_l^{(n)}+2\mathrm{i}lk\frac{\partial\varphi_l^{(n-1)}}{\partial\xi}=n_{-,l}^{(n)}-n_{+,l}^{(n)} \tag{10}$$

where $\sigma_\alpha=T_\alpha/T_-$, i.e. $\sigma_-=1$ and $\sigma_+=\sigma=T_+/T_-$; and $\kappa_\alpha=1$ for $\alpha=-$ and $\kappa_\alpha=\beta$ for $\alpha=+$; recall that $\beta=n_{+,0}/n_{-,0}$.

From the first-order ($n=1$) equations, we obtain

$$\begin{aligned}
&-\mathrm{i}l\omega n_{-,l}^{(1)}+\mathrm{i}lkU_{-,l}^{(1)}=0, && -\mathrm{i}l\omega n_{+,l}^{(1)}+\mathrm{i}lk\beta U_{+,l}^{(1)}=0\\
&-\mathrm{i}l\omega U_{-,l}^{(1)}=\mathrm{i}lk\varphi_l^{(1)}-3\mathrm{i}lkn_{-,l}^{(1)}, && -\mathrm{i}l\omega U_{+,l}^{(1)}=-\mathrm{i}lk\varphi_1^{(1)}-3\mathrm{i}l\sigma k\beta n_{+,1}^{(1)},\\
&-l^2k^2\phi_l^{(1)}=n_{-,l}^{(1)}-n_{+,l}^{(1)},
\end{aligned} \tag{11}$$

from which the following dispersion relation is deduced, for $l=1$

$$\frac{\beta}{\omega^2-3\sigma k^2\beta^2}+\frac{1}{\omega^2-3k^2}=1, \tag{12}$$

as a compatibility requirement. Two real solutions are thus obtained for the frequency square ω^2, defined by

$$\omega_1^2=\frac{1+\beta}{2}+\frac{3}{2}(1+\sigma\beta^2)k^2-\frac{1}{2}\sqrt{9k^4(1-\sigma\beta)^2+6(\beta-1)(\sigma\beta^2-1)k^2+(1+\beta)^2} \tag{13a}$$

and

$$\omega_2^2=\frac{1+\beta}{2}+\frac{3}{2}(1+\sigma\beta^2)k^2+\frac{1}{2}\sqrt{9k^4(1-\sigma\beta)^2+6(\beta-1)(\sigma\beta^2-1)k^2+(1+\beta)^2}. \tag{13b}$$

See that, for all values of β and σ, the lower mode satisfies $\omega_1\to 0$ as $k\to 0$, while the upper mode goes to a finite cutoff frequency $\omega_1\to\sqrt{1+\beta}$, as observed in the experiment by Oohara and Hatakeyama [10].

For small k, these branches behave as

$$\omega_1^2\approx 3\beta(1+\sigma\beta)k^2/(1+\beta), \tag{14a}$$

and

$$\omega_2^2\approx 1+\beta+3(1+\sigma\beta^3)k^2/(1+\beta), \tag{14b}$$

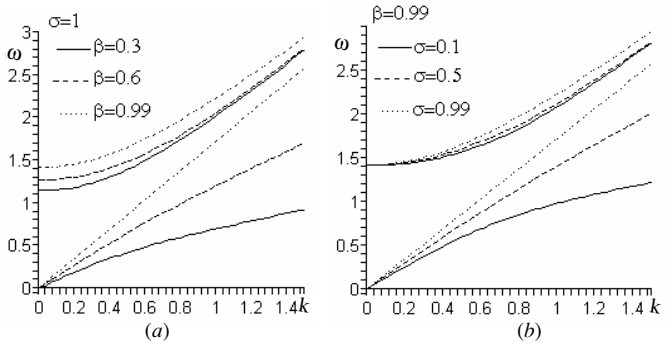

Figure 1. The two dispersion curves defined by equation (13) are depicted, as a frequency ω/ω_p variation versus the reduced wavenumber $k\lambda_D$.

i.e. recovering dimensions,

$$\omega_1^2 \approx 3\beta(1+\sigma\beta)c_s k^2/(1+\beta)$$

and

$$\omega_2^2 \approx (1+\beta)\omega_p^2 + 3(1+\sigma\beta^3)c_s^2 k^2\big/(1+\beta)$$

(setting $\beta = \sigma = 1$, one recovers the pure pair plasma limit formulae which is found in the literature). See that the cutoff frequency $\omega_1 \to \omega_p\sqrt{1+\beta}$ is affected by the pair-species' densities, but not by their temperatures; cf figures 1(*a*) and (*b*). Two characteristic velocities, $c_{0L} = c_s\sqrt{3\beta(1+\sigma\beta)/(1+\beta)}$ and $c_{0U} = c_s\sqrt{3(1+\sigma\beta^3)/(1+\beta)}$ are thus defined. Electrostatic modes in e–p–i plasmas therefore include an *acoustic* dispersion, $\omega_1 \approx \pm c_{oL}k$, and a Langmuir-like optical behaviour $\omega_2 \approx \pm\sqrt{(1+\beta)\omega_p^2 + c_{0U}^2 k^2}$, for small k. For clarity, $\omega_1 = \omega_L$ and $\omega_2 = \omega_U$ will henceforth be referred to as the lower and the upper curve, respectively. Note, for rigour, that the lower branch has been argued to be subject to strong damping, in electron–positron plasmas, due to the phase velocity ω_1/k being close to the sound velocity [36]. However, this may not necessarily be true in e–p–i , thanks to the extra ion component and/or the pair-ion species temperature ratio, which affects the wave front phase velocity. The dispersion laws presented here are in full agreement with (and, in fact, generalize) known experimental [8, 9] and theoretical [3] results for pair plasmas. It may be noted, for the sake of rigor, that the lower dispersion relation cannot exist for an identical positive and negative ion population plasma preparation to see this, set $\beta = \sigma = 1$ in equation (12), a fact which seems to point towards an asymmetry of the pair-ion constituents in the experiment described in [8, 9] (where the acoustic mode was indeed observed).

The two dispersion curves obtained above are depicted in figure 1. We note on the plots the dependence of the dispersion relation on the parameters involved, namely the positive-to-negative ion (or positron-to-electron) density and temperature ratios β and σ. The wave frequency for a fixed wavenumber clearly increases with higher β, i.e. for a lower fixed ion concentration; in other words, the addition of a stationary positive ion component results in lower frequency values and lower phase speeds, for small k; the phase velocity (slope) is also affected—see in figure 1(*a*). The opposite effect should be expected if the stationary ions were negatively charged. On the other hand, higher values of the temperature σ (e.g. hotter positrons, in e–p–i plasma) result in lower frequency values—see in figure 1(*b*). All of these effects are more intense in the lower (acoustic) mode, and only slightly observed in the upper

mode (hence the extreme parameter values considered in figure 1, to depict the change in the curve).

The first-order first harmonic amplitudes are now determined as

$$n^{(1)}_{-,1} = \frac{k^2}{-\omega^2 + 3k^2}\varphi^{(1)}_1, \qquad n^{(1)}_{+,1} = \frac{k^2\beta}{\omega^2 - 3\sigma k^2\beta^2}\varphi^{(1)}_1, \qquad k\beta U^{(1)}_{+,1} = \omega n^{(1)}_{+,1},$$
$$U^{(1)}_{-,l} = \frac{k\omega}{-\omega^2 + 3k^2}\varphi^{(1)}_1, \qquad U^{(1)}_{+,1} = \frac{k\omega}{\omega^2 - 3\sigma k^2\beta^2}\varphi^{(1)}_1. \tag{15}$$

The frequency in these (and all forthcoming) expressions refers to either the lower or the upper branch. Note that these expressions would be meaningless if $\sigma = 1$ and $\beta = 1$ were simultaneously satisfied the denominators would then vanish; cf (13*a*) and (13*b*)); this is not the case here, by assumption.

For the second-order ($n = 2$) equations with $l = 1$ (first harmonics), we deduce the following compatibility condition:

$$\lambda = \frac{\omega}{k} - \frac{1}{k\omega\left[\frac{1}{(\omega^2-3k^2)^2} + \frac{\beta}{(\omega^2-3\sigma k^2\beta^2)^2}\right]}. \tag{16}$$

It is easy to show that $\lambda = v_g(k) = \partial\omega/\partial k$. The real parameter λ therefore denotes the group velocity.

3.2. The nonlinear Schrödinger equation

Proceeding to $n = 2, l = 2$ in combination with $n = 3, 1 = 0, 1$ in equations (8)–(10), we obtain a compatibility condition in the form of the nonlinear Schrödinger equation:

$$\mathrm{i}\frac{\partial\varphi}{\partial\tau} + P\frac{\partial^2\varphi}{\partial\xi^2} + Q\,|\varphi|^2\,\varphi = 0, \tag{17}$$

which describes the slow evolution of the first-order amplitude of the plasma potential perturbation $\varphi \equiv \varphi^{(1)}_1$. The dispersion coefficient P is related to the dispersion curve as $P = \partial^2\omega/2\partial k^2$. Its exact form reads

$$\begin{aligned} P = {} & \frac{(\omega^2 - k\lambda\omega)^2(\omega - k\omega)}{2\omega^2k^2}\left[\frac{\omega^2 + 3k^2}{(\omega^2 - 3k^2)^3} + \frac{\beta(\omega^2 + 3\sigma k^2\beta^2)}{(\omega^2 - 3\sigma k^2\beta^2)^3}\right] \\ & + \frac{3(\omega^2 - k\lambda\omega)^2}{\omega}\left[\frac{1}{(\omega^2 - 3k^2)^3} + \frac{\sigma\beta^3}{(\omega^2 - 3\sigma k^2\beta^2)^3}\right] - \frac{\omega^2 - k\lambda\omega}{2\omega k^2} \\ & - \frac{(\omega^2 - k\lambda\omega)^2\lambda}{k}\left[\frac{1}{(\omega^2 - 3k^2)^3} + \frac{\beta}{(\omega^2 - 3\sigma k^2\beta^2)^3}\right]. \end{aligned} \tag{18}$$

The nonlinearity coefficient Q, which is due to the carrier wave self-interaction, is given by

$$\begin{aligned} Q = {} & -\frac{k^3(2\omega + k\lambda)(\omega^2 - k\lambda\omega)}{2\lambda\omega}\left[\frac{(\omega^2 + 3k^2)}{(\omega^2 - 3k^2)^4} + \frac{\beta(\omega^2 + 3\sigma k^2\beta^2)}{(\omega^2 - 3\sigma k^2\beta^2)^4}\right] \\ & - \frac{3k^4(\omega^2 - k\lambda\omega)}{4\omega}\left[\frac{(\omega^2 + 3k^2)(\omega^2 + k^2)}{(\omega^2 - 3k^2)^5} + \frac{\beta(\omega^2 + 3\sigma k^2\beta^2)(\omega^2 + \sigma k^2\beta^2)}{(\omega^2 - 3\sigma k^2\beta^2)^5}\right] \\ & - \frac{3k^4(\omega^2 - k\lambda\omega)}{4\omega}\left[\frac{(\omega^2 + k^2)[\omega^2 + k^2 + 6k^2(\omega^2 - 3k^2)]}{(\omega^2 - 3k^2)^6}\right. \\ & \left. + \frac{\beta^2(\omega^2 + \sigma k^2\beta^2)[\omega^2 + \sigma k^2\beta^2 + 6\sigma k^2\beta(\omega^2 - 3\sigma k^2\beta^2)]}{(\omega^2 - 3\sigma k^2\beta^2)^6}\right] \end{aligned}$$

$$+\frac{3\beta k^4(\omega^2+k^2)(\omega^2+\sigma k^2\beta^2)(\omega^2-k\lambda\omega)}{2\omega(\omega^2-3k^2)^3(\omega^2-3\sigma k^2\beta^2)^3}+\frac{(2k\lambda\omega+\omega^2+3k^2)(\omega^2-k\lambda\omega)}{2\omega[\lambda^2-3\sigma\beta^2+(\lambda^2-3)\beta]}$$
$$\times\left[\frac{2\omega k^3(\lambda^2-3\sigma\beta^2-3\beta)-k^2\beta\lambda(\omega^2+3k^2)}{\lambda(\omega^2-3k^2)^4}-\frac{4\omega k^3\lambda\beta}{(\omega^2-3k^2)^2(\omega^2-3\sigma k^2\beta^2)^2}\right.$$
$$-\frac{k^2\beta(2\omega^2+3k^2+3\sigma k^2\beta^2)}{(\omega^2-3k^2)^2(\omega^2-3\sigma k^2\beta^2)^2}$$
$$\left.+\frac{2\omega k^3\beta^2(\lambda^2-3\sigma\beta-3)-k^2\beta\lambda(\omega^2+3\sigma k^2\beta^2)}{\lambda(\omega^2-3\sigma k^2\beta^2)^4}\right]. \tag{19}$$

It may be interesting to trace the asymptotic behaviour of these coefficients for small k, i.e. for a large wavelength, compared to the Debye radius. At first we consider low mode. P_L behaves as $P_L \approx -c_{P,L}k$ for small k, while Q_L goes to infinity as $Q_L \approx c_{Q,L}/k$ (the expressions for the quantities $c_{P,L}$ and $c_{Q,L}$ are given in the appendix). The product PQ is therefore negative (prescribing modulational stability, as we shall see) and independent of k, for small k (i.e. in the long-wavelength limit), while $P/Q \propto -k^2$ in the same limit. For the upper mode, P_U goes to a constant as $P_U \sim 3(\sigma^3+1)/(1+\beta)^{3/2} > 0$, while Q_U behaves as $Q_U \sim c_{Q,U}k^2 > 0$ (the expression for $c_{Q,U}$ is given in the appendix). The product PQ is therefore positive (favouring modulational instability, as we will see below) and tends to zero, for small k, while $P/Q \sim k^{-2} > 0$ in the same limit.

4. Modulational instability and envelope excitations

4.1. Modulational stability analysis

The stability analysis of the NLS equation (17) consists in linearizing around the monochromatic wave solution $\psi = \hat{\psi}\,\mathrm{e}^{\mathrm{i}Q|\hat{\psi}|^2\tau}$, i.e. by setting $\hat{\psi} = \hat{\psi}_0 + \varepsilon\hat{\psi}_1$, and then taking the perturbation $\hat{\psi}_1$ to be of the form $\hat{\psi}_1 = \hat{\psi}_{1,0}\,\mathrm{e}^{\mathrm{i}(\hat{k}\xi-\hat{\omega}\tau)}$ (the perturbation wavenumber $\hat{k}$ and frequency $\hat{\omega}$ should be distinguished from the carrier wave quantities k and ω). One thus obtains the dispersion relation $\hat{\omega}^2 = P\hat{k}^2(P\hat{k}^2 - 2Q|\hat{\psi}_0|^2)$. In order for the wave to be stable, the product PQ must be negative. Otherwise, for positive PQ, instability sets in for perturbation wavenumber values below a critical value $\hat{k}_{cr} = \sqrt{2Q/P}|\hat{\psi}_0|$, i.e. for wavelength values above the threshold $\lambda_{cr} = 2\pi/\hat{k}_{cr}$. The maximum instability growth rate $\sigma = |\mathrm{Im}\,\hat{\omega}(\hat{k})|$, i.e. $\sigma_{\max} = |\mathrm{Im}\,\hat{\omega}|_{\hat{k}=\hat{k}_{cr}/\sqrt{2}} = |Q||\hat{\psi}_0|^2$, is achieved for $\hat{k} = \hat{k}_{cr}/\sqrt{2}$.

We draw the conclusion that the instability condition depends only on the sign of the product PQ, which may be studied numerically, relying on the exact expressions derived above.

4.2. Envelope soliton solutions of the NLSE

The localized solutions of the NLSE (17) describe (arbitrary amplitude) nonlinear excitations, in the form of bright and dark (black/grey) envelope solitons. Exact expressions for these envelope structures can be found by substituting with $\varphi = \sqrt{\rho}\exp(i\theta)$ into equation (17), and then separating real and imaginary parts. The final formulae are exposed e.g. in [32, 37], and will therefore only briefly be summarized in the following.

For $PQ > 0$ we find the *bright* envelope soliton:

$$\rho = \rho_0\,\mathrm{sech}^2\left(\frac{\xi-u\tau}{l}\right), \qquad \theta = \frac{1}{2P}\left[u\xi-\left(\Omega+\frac{1}{2}u^2\right)\tau\right]$$

which represents a localized pulse travelling at a speed u and oscillating at a frequency

Ω (at rest). The pulse width l depends on the constant maximum amplitude square ρ_0 as $l = \sqrt{2P/Q\rho_0}$. We note that the maximum amplitude $\sqrt{\rho_0}$ is inversely proportional to the spatial extension l; this is in fact also true in the dark (i.e. black/grey) envelope soliton case (see below).

For $PQ < 0$ we have the *black* envelope soliton

$$\rho = \rho_1 \left[1 - \operatorname{sech}^2\left(\frac{\xi - u\tau}{l'}\right)\right] = \rho_1 \tanh^2\left(\frac{\xi - u\tau}{l'}\right),$$
$$\theta = \frac{1}{2P}\left[u\xi - \left(\frac{1}{2}u^2 - 2PQ\rho_1^2\right)\tau\right],$$

representing a localized region of negative wave density travelling speed u. The pulse width depends on the maximum amplitude square ρ_1 via $l' = \sqrt{|2P/Q\rho_1|}$.

Finally, for $PQ < 0$, one also obtains the *grey envelope soliton* excitation

$$\rho = \rho_2 \left[1 - a^2 \operatorname{sech}^2\left(\frac{\xi - u\tau}{l''}\right)\right],$$

which also represents a localized region of negative wave density, θ_{10} is a constant phase, s denotes the product $s = \text{sign } P \times \text{sign}(u - V_0)$. In comparison to the *black* soliton above, note that apart from the maximum amplitude $\sqrt{\rho_2}$, which is now finite everywhere, the pulse width of this grey-type excitation: $l'' = (1/a)\sqrt{2|P/Q\rho_2|}$, now also depends on the dimensionless parameter a, which is given by $a^2 = 1 + (u - V_0)^2/(2PQ\rho_2) \leqslant 1$ (for $PQ < 0$), an independent parameter representing the modulation depth ($0 < a \leqslant 1$). V_0 is an independent real constant which satisfies the condition: $V_0 - \sqrt{2|PQ|\rho_2^2} \leqslant u \leqslant V_0 + \sqrt{2|PQ|\rho_{2^2}}$; for $V_0 = u$, we have $a = 1$ and thus recover the *black* soliton presented in the previous paragraph.

5. Numerical analysis

Summarizing the previous section, we have seen that the sign of the coefficient product PQ determines the stability profile of ES waves and the type of envelope excitations (negative/positive for stability/instability and bright/dark type envelope solitons), while the ratio P/Q determines the spatial extension of the localized envelope structures for a given maximum amplitude (and vice versa), in an inverse-proportional manner. We may now investigate the numerical value of these quantities in terms of the relevant physical parameters, namely the positron-to-electron (or positive-to-negative ion) density and temperature ratio(s), $\beta = n_{+,0}/n_{-,0}$ and $\sigma_+ = \sigma = T_+/T_-$, respectively.

The results of the calculations for fixed values of σ and different values of β for the lower mode (acoustic branch) are shown in figures 2(*a*) and (*b*), for small k (large wavelengths), and in figures 3(*a*) and (*b*) for higher k. We may nevertheless admit, for rigor, that figures 3(*a*) and (*b*) are invalidated by Landau damping, which is expected to be dominant for large k (where the ES wave phase velocity is comparable to the ion thermal velocity), and are thus only provided for indicative purposes. We find out that both dark (grey or black, for $PQ < 0$) and bright (for $PQ > 0$) excitations may occur. The former dominate the large wavelength (small k) region, while the latter exist in a bounded range of values for shorter wavelengths in which $PQ > 0$ (namely, from a zero-nonlinearity point $k = k_{\text{ZNP}} > 0$, where $Q = 0$ or $P/Q \to \pm\infty$, up to a zero-dispersion point, $k = k_{\text{ZDP}}$, say ZDP, where $P = 0$). Upon careful inspection of figure 2(*a*) and figure 3(*a*), one observes that the range of positive PQ values (hence instability) increases and shifts to higher values of k as β increases, for a fixed σ. As figure 2(*b*) shows, the width of grey and dark excitations increases as k increases until $k = k_{\text{ZNP}}$, while that of bright excitations decreases as k increases from $k = k_{\text{ZNP}}$ up to $k = k_{\text{ZDP}}$. For a fixed value of

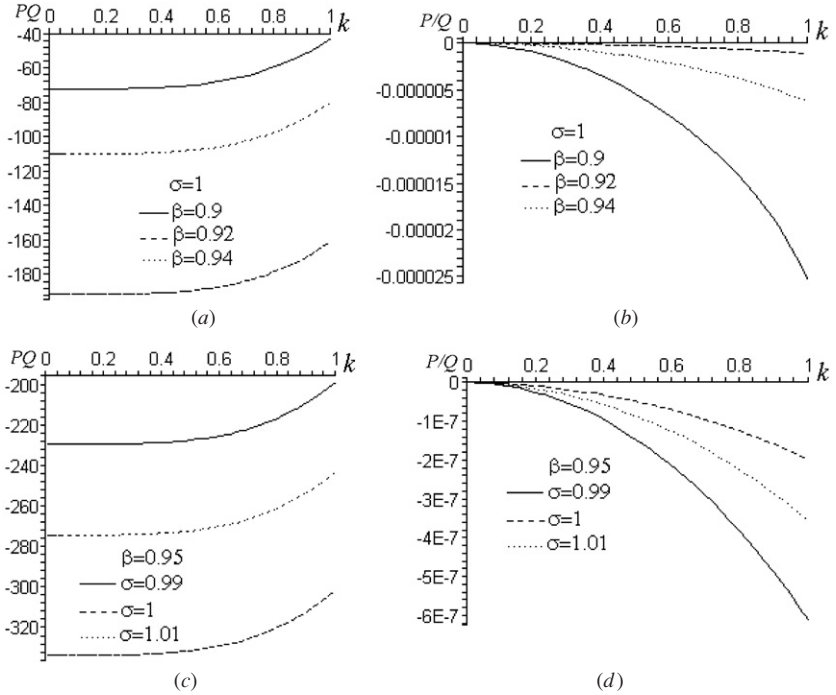

Figure 2. The NLSE coefficient product PQ ((*a*) and (*c*)) and ratio P/Q ((*b*) and (*d*)) corresponding to the lower dispersion branch ω_1 are depicted against the reduced wavenumber $k\lambda_D$ (in abscissa everywhere). Here ((*a*) and (*b*)) $\sigma = 1$, and different values of β are considered; ((*c*) and (*d*)) $\beta = 0.95$, and σ varies.

k, the width of dark (bright) excitations is shown to decrease (increase), for a given maximum amplitude, as the density ratio increases. Admittedly, as stated above, high values of k are rather excluded physically, due to Landau damping (which is inevitably omitted in a fluid plasma description), so we need not pursue this analysis any further. Also, we note that the NLSE-based analysis breaks down near the ZDP, where higher-order nonlinearity takes over (this is a well-known phenomenon in nonlinear optics).

Considering a fixed value of β for different values of σ, for the lower mode, we have obtained figures 2(*c*) and (*d*) and figure 3(*c*) and (*d*). The qualitative aspects of the above analysis are also valid in this case. Thus, increasing the density of positrons (or positive ions) with respect to their electron (or negative ion) counterpart results in an increase in the wavenumber instability threshold, and therefore slightly favours stability. For a fixed value of k, the width of dark (bright) excitations is shown to decrease (increase), for a given maximum amplitude, as the temperature ratio increases.

Let us consider the upper mode (optical dispersion branch). The results of the calculation for a fixed temperature ratio σ and different values of the density ratio β (or, respectively, fixed β and varying σ) for this mode are shown in figures 4(*a*) and (*b*) (or, respectively, figures 4(*c*) and (*d*)). Both dark (for $PQ < 0$) and bright (for $PQ > 0$) excitations can exist for this mode. Note, however, that the qualitative profile is reversed, with respect to the lower mode: here, bright excitations and modulational instability occur for small k, in fact from zero up to a threshold $k = k_{cr}$ (see that $Q \to \pm\infty$ as $k \to k_{cr}$), while dark excitations (and modulational stability of the envelope) occur for larger k, after $k = k_{cr}$. As the width of bright

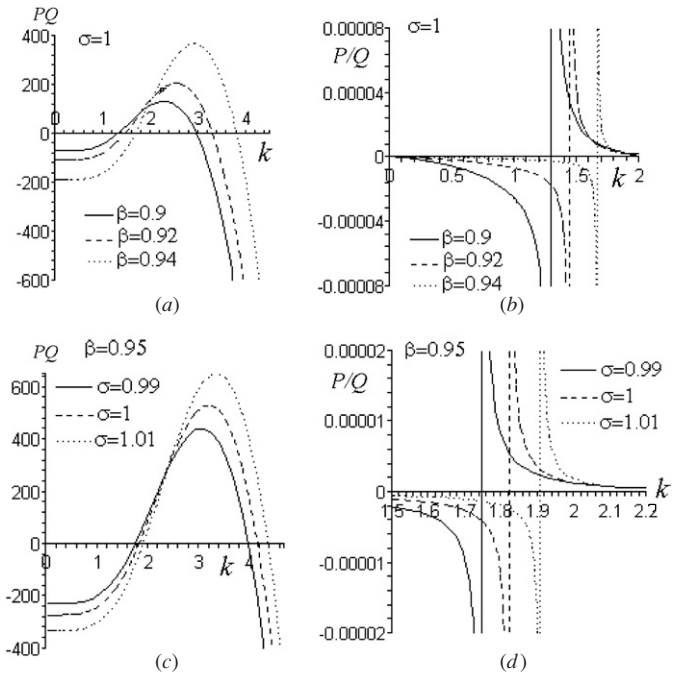

Figure 3. The same as in figure 2, for higher wavenumber k values.

excitations becomes narrower as k increases from zero up to $k = k_{cr}$, where it reaches zero. Beyond $k = k_{cr}$, only stable envelopes may propagate, in the form of dark-type envelope solitons; the corresponding localized envelope width increases up to a maximum value, and then decreases as k increases (still, these low wavelength results are to be interpreted with precaution). Upon careful inspection of figures 3(a) and (c), one observes that k_{cr} shifts to larger values as either σ or β increases.

Summarizing, we conclude that the lower (acoustic) mode is generally stable, for realistic large wavelength situations (see figures 2(a) and (d)) and may propagate in the form of a dark-type envelope soliton (i.e. a potential dip, a void). On the other hand, the upper (Langmuir-like) mode is modulationally unstable (see figures 4(a) and (d)), and may favour the formation of bright-type envelope soliton (pulse) modulated wavepackets at low wavenumbers. We remark that, once the potential perturbation is determined by the NLSE (17), the density and velocity variations are given by expressions (15); it may be checked that the two fluids (negative and positive ions) are subject to a perturbation of opposite sign to one-another: an increase in the number density (or the velocity) of one entails a depletion (or a slow-down) in the other, as may be seen in equation (15). Finally, comparing to the 'pure' e–p (or pair–ion) plasma, which was presented in [34, 35], we note that the qualitative profile depicted above remains similar (despite an analytical complication discussed in [35]). It should be pointed out, however, that all relevant wavenumber thresholds are increased in our case here; this implies that the presence of ions in e–p plasma (respectively: charged defects, say, in pair-ion plasma) results in a significant increase of the wavenumber range where the lower (acoustic) mode is stable (favouring dark solitons, i.e. holes/voids) and/or where the upper (Langmuir-like) mode is unstable (favouring bright solitons, i.e. pulses).

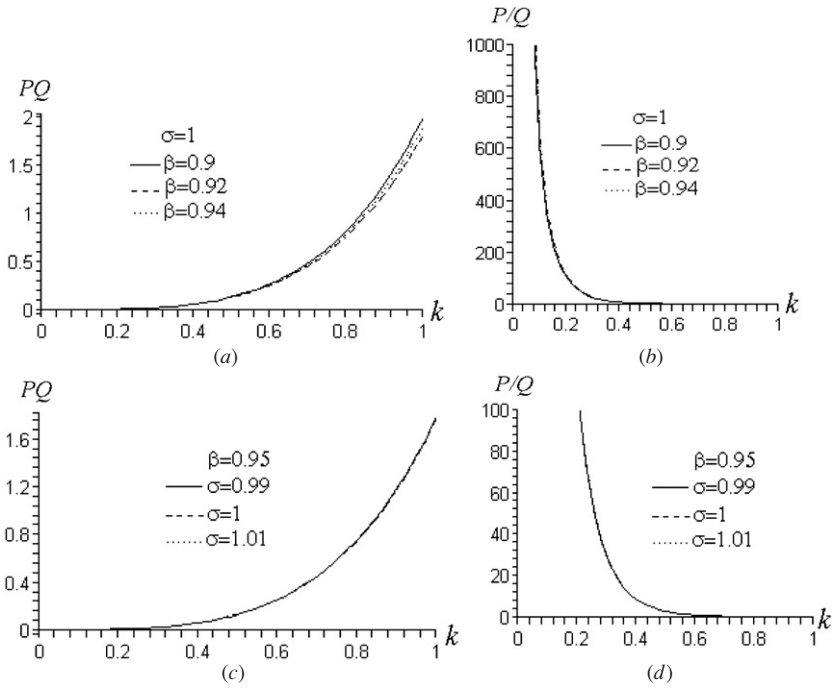

Figure 4. The NLSE coefficient product PQ ((*a*) and (*c*)) and the ratio P/Q ((*b*) and (*d*)) corresponding to the lower dispersion branch ω_2 are depicted against the reduced wavenumber $k\lambda_D$ (in abscissa everywhere). Here ((*a*) and (*b*)) $\sigma = 1$, and different values of β are considered; ((*c*) and (*d*)) $\beta = 0.95$, and σ varies.

6. Conclusions

In this paper, we have investigated the nonlinear propagation of electrostatic wavepackets in e–p–i plasmas, by employing a two-fluid plasma model. The results equally apply in the case of a pair-ion plasma, in the presence of a small fraction of uniform and stationary charged particles (e.g. dust). Electrostatic mode propagation parallel to the external magnetic field was considered. The temperature ratio between the two species has been left arbitrary in the analysis, although a natural choice of unity was implicitly focused upon. Two distinct electrostatic modes were obtained, namely a quasi-thermal lower mode and a Langmuir-like optic-type upper one which is the case for pure pair plasmas, in agreement with previous experimental observations confirmed by theoretical studies of equal-temperature pair plasmas. Considering small yet weakly nonlinear deviations from equilibrium, and adopting a multiple scale technique, the basic set of model equations was reduced to a nonlinear Schrödinger equation for the slowly varying electric field perturbation amplitude.

The analysis revealed that the stability range of lower (acoustic) mode increases as the positive ion (or positron) to negative ion (or electron) ion density ratio β increases. The lower mode may propagate in the form of a dark-type envelope soliton (i.e. a potential dip, or a void) which modulates a carrier wave. On the other hand, the upper mode is mostly modulationally unstable, and may yet favour the formation of bright-type envelope soliton (pulse) modulated wavepackets at small wavenumbers. As mentioned above, these results depend on the temperature ratio, as one may see in figures 2–4. In specific, one may anticipate

that a local coexistence of positive ions (or positrons) with a colder, say, population of negative ions (or electrons), namely $\sigma < 1$ ($\sigma > 1$), may critically affect the stability profile of electrostatic modes, for instance by stabilizing the lower mode, or by destabilizing the upper mode.

It should be added, for rigour, that our results on the lower mode are somewhat invalidated by Landau damping, which will dominate if the pair-ion temperatures are equal. However, we speculate that allowing for $T_+ \neq T_-$, and hence modifying the group velocity (see the slope in figure 1(*b*)) may decrease Landau damping and allow ES oscillations to survive. Preliminary theoretical calculations in this direction are currently carried out and should be reported soon.

These results are relevant to recent observations of electrostatic waves in pair-ion (fullerene) plasmas. In particular, one may anticipate doping fullerene plasmas with charged massive defects (or dust particles), in order to tune the characteristic features of plasma modes. This analysis may also be relevant to modulated electron–positron–ion plasma radio emission in pulsar magnetospheres. Our predictions may be investigated, and will hopefully be confirmed, by appropriately designed experiments.

Acknowledgments

The work of one of us (IK) was partially supported by the Deutsche Forschungsgemeinschaft (Bonn, Germany) through the Sonderforschungsbereich (SFB) 591—Universelles Verhalten Gleichgewichtsferner Plasmen: Heizung, Transport und Strukturbildung. IK wishes to thank Professor F Verheest for a number of enlightening discussions on pair plasmas. He also acknowledges the hospitality of Sterrenkundig Observatorium (Universiteit Gent, Belgium), where this work was completed. AE-K, IK and PKS gratefully acknowledge the hospitality offered by the Abdus Salam International Centre for Theoretical Physics, during the International Workshop on Frontiers of Plasma Science (August 2006), during which part of this work was carried out. The assistance offered by the anonymous referee is gratefully acknowledged.

Appendix

$$c_{P,L} = \frac{9\sqrt{3}(\sigma\beta^2 - 1)^2\sqrt{\frac{\beta(1+\sigma\beta)}{1+\beta}}}{2[1 + (2+\sigma)\beta + (1+2\sigma)\beta^2 + \sigma\beta^3]}$$

$$\begin{aligned} C_{Q,L} = \Bigg(& (9\sqrt{3}\,\sigma^2\beta^9 + 18\sqrt{3}\,\sigma^2\beta^8 + 24\sqrt{3}\,\beta^8\sigma + 54\sqrt{3}\,\beta^7\sigma + 26\sqrt{3}\,\sigma^2\beta^7 + 16\sqrt{3}\,\beta^7) \\ & + 40\sqrt{3}\,\beta^6 + 84\sqrt{3}\,\beta^6\sigma + 32\sqrt{3}\,\sigma^2\beta^6 + 65\sqrt{3}\,\beta^5 + 21\sqrt{3}\,\sigma^2\beta^5 + 116\sqrt{3}\,\beta^5\sigma \\ & + 14\sqrt{3}\,\sigma^2\beta^4 + 104\sqrt{3}\,\sigma\beta^4 + 90\sqrt{3}\,\beta^4 + 82\sqrt{3}\,\beta^3 + 8\sqrt{3}\,\sigma^2\beta^3 + 78\sqrt{3}\,\sigma\beta^3 \\ & + 56\sqrt{3}\,\beta^2 + 44\sqrt{3}\,\sigma\beta^2 + 8\sqrt{3}\,\sigma\beta + 29\sqrt{3}\,\beta + 6\sqrt{3})\sqrt{\frac{\beta(1+\sigma\beta)}{\sigma+\beta}}\Bigg) \Bigg/ \\ & (-1296\sigma^4\beta^{10} + 1944\sigma^3\beta^8 - 1296\sigma^2\beta^6 + 324\sigma^5\beta^{12} - 1296\sigma^3\beta^9 \\ & + 1944\sigma^2\beta^7 - 1296\beta^5\sigma + 324\sigma^4\beta^{11} + 324\sigma\beta^4 - 324\beta^3) \end{aligned}$$

$$\begin{aligned} C_{Q.U} = & \frac{1}{3(1+\beta)^{(29/2)}\sigma\beta + 3(1+\beta)^{(29/2)}} \\ & \times (2\beta^{13} + 26\beta^{12} + 156\beta^{11} + 572\beta^{10} + 1430\beta^9 + 2574\beta^8 \\ & + 3432\beta^7 + 3432\beta^6 + 2574\beta^5 + 1430\beta^4 + 572\beta^3 + 156\beta^2 + 26\beta + 2). \end{aligned}$$

References

[1] Chen F F 1974 *Introduction to Plasma Physics* (New York: Plenum) p 121
Hall J O and Shukla P K 2005 *Phys. Plasmas* **12** 084507
[2] Iwamoto N 1993 *Phys. Rev.* E **47** 604
[3] Zank G P and Greaves R G 1995 *Phys. Rev.* E **51** 6079
[4] Bulanov S S 2004 *Phys. Rev.* E **69** 036408
[5] Kluger Y, Eisenberg J M, Svetitsky B, Cooper F and Mottola E 1991 *Phys. Rev. Lett.* **67** 2427–30
[6] Prozorkevich A V, Reichel A, Smolyansky S A and Tarakanov A V 2004 *Proc. SPIE* **5476** 68–72
[7] Greaves R G, Tinkle M D and Surko C M 1994 *Phys. Plasmas* **1** 1439
[8] Oohara W and Hatakeyama R 2003 *Phys. Rev. Lett.* **91** 205005
[9] Oohara W, Date D and Hatakeyama R 2005 *Phys. Rev. Lett.* **95** 175003
[10] Hatakeyama R and Oohara W 2005 *Phys. Scr.* **116** 101
[11] Rees M J 1983 *The Very Early Universe* Cambridge: Cambridge University Press)
[12] Miller H R and Witta P J 1987 *Active Galactic Nuclei* (Berlin: Springer) p 202
[13] Michel F C 1982 *Rev. Mod. Phys* **54** 1
[14] Greaves R G and Surko C M 1995 *Phys. Rev. Lett.* **75** 3847
[15] Berezhiani V I, Tskhakaya D D and Shukla P K 1992 *Phys. Rev.* A **46** 6608
[16] Surko C M, Levelhal M, Crane W S, Passne A and Wysocki F 1986 *Rev. Sci. Instrum* **57** 1862
[17] Surko C M and Murphay T 1990 *Phys. Fluid* B **2** 1372
[18] Berezhiani V I, El-Ashry M Y and Mofiz U A 1994 *Phys. Rev.* E **50** 000448
[19] Berezhiani V I and Mahajan S M 1995 *Phys. Rev.* E **52** 001968
[20] Mahajan S M, Berezhiani V I and Miklaszewski R 1998 *Phys. Plasmas* **5** 3264
[21] Eliasson B and Shukla P K 2005 *Phys. Plasmas* **12** 104501
[22] Bulanov S S, Fedotov A M and Pegoraro F 2005 *Phys. Rev.* E **71** 016404
[23] Krall N A and Trivelpiece A W 1973 *Principles of Plasma Physics* (NewYork: McGraw-Hill)
[24] Stix T 1992 *Waves in Plasmas* (New York: American Institute of Physics)
[25] Popel S I, Vladimirov S V and Shukla P K 1995 *Phys. Plasmas* **2** 716
[26] Nejoh Y N 1997 *Aust. J. Phys.* **50** 309
[27] Mahmood S, Mushtaq A and Saleem H 2003 *New J. Phys.* **5** 28.1
[28] Mahmood M A, Mahmood S, Mirza A M and Saleem H 2005 *China. Phys. Lett* **22** 632
[29] Sulem P and Sulem C 1999 *Nonlinear Schrödinger Equation* (Berlin: Springer)
[30] Taniuti T and Yajima N 1969 *J. Math. Phys.* **10** 1369
[31] Asano N, Taniuti T and Yajima N 1969 *J. Math. Phys.* **10** 2020
[32] Kourakis I and Shukla P K 2005 *Nonlinear Proc. Geophys.* **12** 407
[33] Salahuddin M, Saleem H and Saddiq M 2002 *Phys. Rev.* E **66** 036407
[34] Amiranashvili Sh. G and Ignatov A M 1995 *Plasma Phys. Rep.* **21** 364
[35] Kourakis I, Esfandyari-Kalejahi A, Mehdipoor M and Shukla P K 2006 *Phys. Plasmas* **13** 052117
[36] Tsytovich V and Wharton C B 1978 *Commun. Plasma Phys. Cont. Fusion* **4** 91
[37] Fedele R 2002 *Phys. Scr.* **65** 502
Fedele R and Schamel H 2002 *Eur. Phys. J.* B **27** 313

Nonlinear perpendicular propagation of ordinary mode electromagnetic wave packets in pair plasmas and electron-positron-ion plasmas

I. Kourakis
Universiteit Gent, Sterrenkundig Observatorium, Krijgslaan 281, B-9000 Gent, Belgium and Institut für Theoretische Physik, Lehrstuhl IV: Weltraum-und Astrophysik, Ruhr-Universität, Bochum, D-44780 Bochum, Germany

F. Verheest
Universiteit Gent, Sterrenkundig Observatorium, Krijgslaan 281, B-9000 Gent, Belgium and School of Physics, University of KwaZulu-Natal, Private Bag X54001, Durban 4000, South Africa

N. F. Cramer
School of Physics, The University of Sydney, New South Wales 2006, Australia

(Received 5 December 2006; accepted 3 January 2007; published online 28 February 2007)

The nonlinear amplitude modulation of electromagnetic waves propagating in pair plasmas, e.g., electron-positron or fullerene pair-ion plasmas, as well as three-component pair plasmas, e.g., electron-positron-ion plasmas or doped (dusty) fullerene pair-ion plasmas, assuming wave propagation in a direction perpendicular to the ambient magnetic field, obeying the ordinary (O-) mode dispersion characteristics. Adopting a multiple scales (reductive perturbation) technique, a nonlinear Schrödinger-type equation is shown to govern the modulated amplitude of the magnetic field (perturbation). The conditions for modulation instability are investigated, in terms of relevant parameters. It is shown that localized envelope modes (envelope solitons) occur, of the bright- (dark-) type envelope solitons, i.e., envelope pulses (holes, respectively), for frequencies below (above) an explicit threshold. Long wavelength waves with frequency near the effective pair plasma frequency are therefore unstable, and may evolve into bright solitons, while higher frequency (shorter wavelength) waves are stable, and may propagate as envelope holes. © *2007 American Institute of Physics*. [DOI: 10.1063/1.2446373]

I. INTRODUCTION

Pair-plasmas (p.p.), i.e., plasmas consisting of negatively and positively charged particles bearing the same mass and (absolute) charge, have been gathering increasing interest among plasma researchers in the last years. Magnetized electron-positron (e-p) plasmas exist in pulsar magnetospheres,[1–5] in bipolar outflows (jets) in active galactic nuclei,[6] at the center of our own galaxy,[7] in the early universe,[8] and in inertial confinement fusion schemes using ultraintense lasers.[9] Nonrelativistic pair plasmas have been created in experiments.[10] Recently, Helander and Ward[11] discussed the possibility of pair production in large tokamaks due to collisions between multi-MeV runaway electrons and thermal particles. Remarkably, *pair plasmas* (p.p.), i.e., plasmas composed of (two populations of) fully ionized particles with same mass and absolute charges of opposite charge polarity (+/−), have recently been created in the laboratory[12] by creating a large ensemble of fullerene ions (C_{60}^{+} and C_{60}^{-}, in equal numbers), thus allowing for a study of p.p. properties with no concern for mutual annihilation (recombination), which limits e-p plasma lifetime.

The physics of pair plasmas is substantially different from that of electron-ion (e-i) plasmas, since the large time and space scale separation among constituents (due to the large ion-to-electron mass ratio, in an e-i plasma)[13–15] is simply absent in a pair plasma (where pair ions bear equal masses).[16,18] In magnetized pair plasma, besides the electrostatic upper-hybrid waves, we have the perpendicularly propagating ordinary and extraordinary modes as well as magnetic field-aligned electromagnetic (EM) waves, featuring a linear polarization. Remarkably, no Faraday rotation exists in p.p. Iwamoto[16] has presented an elegant kinetic description of numerous linear collective modes in a nonrelativistic pair magnetoplasma. Stewart and Laing[17] presented a study of normal p.p. modes via a multifluid description. Zank and Greaves[18] have discussed the linear properties of various electrostatic (ES) and electromagnetic (EM) modes in unmagnetized and in magnetized pair plasmas, and also considered two-stream instability and nonenvelope solitary wave solutions. Linear p.p. modes and associated instabilities have been investigated from a kinetic-theoretical point of view in Refs. 19 and 20.

Nonlinear excitations in pair-plasmas have been studied quite extensively. Large amplitude structures have been modeled via the pseudopotential (see, e.g., in Refs. 21 and 22, and references therein) (and associated, e.g., Bernoulli quasifluid)[23] approach(es), while the Korteweg-deVries (KdV) picture has also been established in the large wavelength limit.[21,24] Modulated ES modes in p.p. (Ref. 25) have also been studied, assuming amplitude modulation parallel to the wave propagation direction. e-p-i plasmas have also been studied, in this direction, with respect to low (ion-acoustic)[26] and higher frequency[27] ES modes; those investigations were recently extended by including modulation

obliqueness effects.[28] Magnetic field-aligned nonlinear Alfvén waves in an ultrarelativistic pair plasma have been investigated by Sakai and Kawata[29] and Verheest.[30] Zhao *et al.*[31] have performed three-dimensional electromagnetic particle simulations of nonlinear Alfvén waves in an electron-positron magnetoplasma. EM p.p. wave modulation due to ponderomotive coupling to slow ES plasma perturbations was considered by Cattaert *et al.*[32]

In this article, we aim at investigating the occurrence of localized EM envelope modes, in relation to pair plasmas. In particular, we shall consider a plasma consisting of two pair ion species (e.g., electrons and positrons, or positive and negative ions in fullerene plasmas), possibly in the presence of a third massive (immobile) background species; this latter particle type may account for ions in e-p-i plasmas or, e.g., for charged massive defects ("dust") in, say, "doped" pair plasmas. We anticipate the existence of modulated localized structures in p.p., related to the mechanism of modulation instability; this term describes the wave amplitude tendency to localize its energy, due to intrinsic medium nonlinearity, either until collapse, or potentially forming stable localized envelope structures, which are distinct from nontopological solitons, e.g., of the KdV type. Although a direct extrapolation from a general multifluid approach (upon setting $m_1=m_2$ therein) may sometimes be legitimate (cf. Refs. 33 and 34), no systematic theory has so far been presented for modulated EM wave packets in pair plasmas. Our purpose is to partially fill this gap. In this study, we shall focus on the O-mode, which is an EM mode propagating in a direction perpendicular to the ambient magnetic field. The dispersion characteristics of the O-mode do not depend on the magnetic field, and are not modified in p.p. (as compared to e-i plasmas), which makes them an appropriate candidate for a tractable modulated EM wave model.

The layout of this article is the following: The model is presented in Sec. II. In Sec. III, perturbation theory is employed and shown to lead to a nonlinear Schrödinger-type (NLS) equation for the wave amplitude. In Sec. IV, the linear stability of the wave envelope is discussed, while the occurrence of envelope solitons is shown in Sec. V, and numerically investigated in Sec. VI. Our results are then summarized in Sec. VII.

II. THE MODEL

We consider a multicomponent collisionless plasma embedded in a uniform magnetic field $\mathbf{B_0}$. The plasma is composed of positive ions (mass m_1, charge $q_1=s_1Z_1e$; here referred to as species 1) and negative ions, or electrons (mass $m_2=m$, charge $q_2=s_2Z_2e$; aka species 2). We have defined the charge state(s) Z_j $(j=1,2)$, the charge sign $s_j=q_j/|q_j|=\pm 1$, and the absolute electron charge e; we shall denote the respective equilibrium number densities by $n_{j,0}$. The pair-plasma limit is recovered from this model, upon setting $Z_1=Z_2=Z$ and $m_1=m_2=m$, at any step. In particular, we aim at modelling e-p plasmas (yet neglecting annihilation) or pair-(e.g., fullerene-) ion [viz. 1 (2)$=C_{60}^{+(-)}$], for $Z=1$. The general notation (i.e., indices $j=1,2$) may, however, be retained, where appropriate. A third species is potentially present, bearing a charge $q_3=s_3Z_3e$ (here $s_3\pm 1$) and a (large) mass $m_3\gg m_{1/2}$, so that it may be considered to be immobile, at the (high) evolution scales of interest. This species models ions $(m_i\gg m_e)$ in e-p-i plasmas (neglecting annihilation), or, better, charged massive defects (dust) in "doped" p.p. Naturally, the "pure" p.p. limit is recovered in the algebra, by setting the third species density $n_3=n_{3,0}=$cst. to zero, at every step.

We consider the (two-) fluid plasma density and momentum equations:

$$\frac{\partial n_j}{\partial t}+\nabla\cdot(n_j\mathbf{u}_j)=0, \tag{1}$$

$$\frac{\partial \mathbf{u}_j}{\partial t}+\mathbf{u}_j\cdot\nabla\mathbf{u}_j=\frac{q_j}{m_j}(\mathbf{E}+\mathbf{u}_j\times\mathbf{B}), \tag{2}$$

where n_j and $\mathbf{u}_j$ denote the density and the mean (fluid) velocity of species j $(=1,2)$. The (total) electric and magnetic fields, $\mathbf{E}$ and $\mathbf{B}$, respectively, obey Maxwell's laws:

$$\frac{\partial \mathbf{B}}{\partial t}=-\nabla\times\mathbf{E}, \tag{3}$$

$$\frac{1}{c^2}\frac{\partial \mathbf{E}}{\partial t}=\nabla\times\mathbf{B}-\mu_0\sum_j n_jq_j\mathbf{u}_j. \tag{4}$$

The electric field $\mathbf{E}$ obeys Poisson's equation

$$\epsilon_0\nabla\cdot\mathbf{E}=e[Z(n_+-n_-)+s_3n_3Z_3] \tag{5}$$

(setting $n_{1/2}=n_{+/-}$, for clarity), while the magnetic field satisfies Gauss' law

$$\nabla\cdot\mathbf{B}=0. \tag{6}$$

The right-hand side (RHS) of Poisson's Eq. (5) is assumed to cancel at equilibrium (only), i.e.,

$$n_{+,0}-n_{-,0}+s_3n_3Z_3/Z=0. \tag{7}$$

We underline the fact that no *a priori* assumption is made on the (conservation of) charge neutrality (or density balance) during dynamical evolution in time (off equilibrium). Notice that the density of the third species tunes the positive-to-negative density ratio at equilibrium, say $r=n_{+,0}/n_{-,0}$, in fact towards values higher (lower) than unity for negative (positive, respectively) third species charge polarity, i.e., if $s_3=-1$ $(+1)$, since (7) implies

$$r=\frac{n_{+,0}}{n_{-,0}}=1-s_3\frac{Z_3}{Z}\frac{n_3}{n_{-,0}}. \tag{8}$$

Retain, in the following, that the (square root of the) ratio r also essentially expresses the ratio among the plasma frequencies $\omega_{p,j}=(n_{j,0}Z_j^2e^2/\epsilon_0m_j)^{1/2}$ (for $j\in\{1,2\}\equiv\{+,-\}$) of the pair constituents, viz. $r=n_{+,0}/n_{-,0}=\omega_{p,+}^2/\omega_{p,-}^2$, so that the existence of the third background species will (only) be reflected in the algebra to follow, via the disparity among $\omega_{p,+}$ and $\omega_{p,-}$ (the pure p.p. limit is recovered by setting $\omega_{p,+}=\omega_{p,-}$, at every step).

The system of Eqs. (1)–(4) form a closed system of scalar evolution equations, for the elements of the state vector $\mathbf{S}=(n_1,u_{1,x/y/z};n_2,u_{2,x/y/z};E_{x/y/z};B_{x/y/z})$. Our aim is to use Eqs.

(1)–(4) as an analytical basis for a perturbative description of the evolution of the system's state; at every stage, Eqs. (5) and (6) are satisfied, if initially valid.

To simplify the calculation, we shall assume that the direction of wave propagation defines the axis x, implying a wave number $\mathbf{k}=k\hat{x}$ for linear waves, and that the external magnetic field $\mathbf{B}_0$ determines the z axis, i.e., $\mathbf{B}_0=B_0\hat{z}$ (here $\hat{x}$, $\hat{y}$, $\hat{z}$ denote the unit vectors along the respective directions). All quantities are assumed to vary along the direction of propagation, i.e., $\nabla\rightarrow\partial/\partial x$ (thus $\nabla\times\cdot$ is $\hat{x}\times\partial\cdot/\partial x$ here). Notice that a static magnetic field component along the direction of propagation is prescribed by Eqs. (6) and (the x component of) (3), so that $B_x=0$ is satisfied here, at all times. The analytical model (and frame) adopted here agrees (for $\theta=\pi/2$ therein) with the oblique propagation picture described in Refs. 22 and 24, and also in Ref. 33, for parallel propagation in multicomponent plasmas (i.e., for $\theta=\pi/2$).

III. DERIVATION OF AN EVOLUTION EQUATION FOR THE EM WAVE AMPLITUDE DYNAMICS

A. Perturbative analysis: The analytical framework

We shall adopt a version of the *reductive perturbation* technique,[35] which was first applied in the study of electron plasma waves[35] and electron-cyclotron waves,[36] more than three decades ago. In order to study the nonlinear (amplitude) modulational stability profile of these electrostatic waves, we consider small deviations from the equilibrium state $\mathbf{S}^{(0)}=(n_{1,0},\mathbf{0};n_{2,0},\mathbf{0};\mathbf{0};\mathbf{B}_0)^T$, i.e. $\mathbf{S}=\mathbf{S}^{(0)}+\epsilon\mathbf{S}^{(1)}+\epsilon^2\mathbf{S}^{(2)}+\cdots$, where $\epsilon\ll 1$ is a (real) smallness parameter. We assume that

$$S_j^{(n)}=\sum_{l=-\infty}^{\infty}S_j^{(n,l)}(X,T)\exp[il(kx-\omega t)],$$

where the condition $S_j^{(n,-l)}=S_j^{(n,l)*}$ holds, for reality. The wave amplitude is thus allowed to depend on the stretched (*slow*) coordinates of space $X=\{\epsilon^n x,\ n=1,2,\ldots\}=\{X_1,X_2,\ldots\}$ and time $T=\{\epsilon^n t,\ n=1,2,\ldots\}=\{T_1,T_2,\ldots\}$ (viz. $X_1=\epsilon x$, $X_2=\epsilon^2 x$, and so forth; same for time), to be distinguished from the (fast) carrier variables x ($\equiv X_0$) and t ($\equiv T_0$). It may be rigorously shown in the following (cf. compatibility requirements at order ϵ^2) that this scheme is tantamount to the assumption $X=\epsilon(x-\lambda t)$ and $T=\epsilon^2 t$ in original works,[35] where the velocity λ is interpreted as the *group velocity*, i.e., $\lambda=v_g=\omega'(k)$. According to the above considerations, we set:

$$\frac{\partial}{\partial t}\Psi_l^{(n)}e^{il\phi}=\left(-il\omega\Psi_l^{(n)}+\epsilon\frac{\partial\Psi_l^{(n)}}{\partial T_1}+\epsilon^2\frac{\partial\Psi_l^{(n)}}{\partial T_2}\right)e^{il\phi}+\mathcal{O}(\epsilon^3),$$

$$\nabla\Psi_l^{(n)}e^{il\phi}=\left(+ilk\Psi_l^{(n)}+\epsilon\frac{\partial\Psi_l^{(n)}}{\partial X_1}+\epsilon^2\frac{\partial\Psi_l^{(n)}}{\partial X_2}\right)e^{il\phi}+\mathcal{O}(\epsilon^3), \tag{9}$$

for any lth phase harmonic amplitude $\Psi_l^{(n)}$ among the components of $\mathbf{S}^{(n)}$. We have defined the carrier (basic harmonic) phase $\phi\equiv kx-\omega t$.

By inserting the above ansatz into Eqs. (1)–(4), one obtains a set of (coupled) reduced evolution equations, which must be solved in each perturbation order $\sim\epsilon^n$ for the lth harmonic amplitudes $S_j^{(n,l)}$ of the state variables (here, $l=-n,-n+1,\ldots,n-1,n$). Although particularly lengthy, the calculation is perfectly straightforward, so unnecessary details will be omitted in the following.

B. First order dynamics ($n=1$): Linear EM waves

The first-order equations describe the dynamics of a *linear* solution of the system of Eqs. (1)–(4) which, for $n=l=1$, lead to the system of equations

$$-\omega n_j^{(1,1)}+n_{j,0}ku_{j,x}^{(1,1)}=0, \tag{10}$$

$$\omega\mathbf{u}_j^{(1,1)}=i\frac{q_j}{m_j}(\mathbf{E}^{(1,1)}+\mathbf{u}_j^{(1,1)}\times\mathbf{B}_0), \tag{11}$$

$$\omega\mathbf{B}^{(1,1)}=\mathbf{k}\times\mathbf{E}^{(1,1)}, \tag{12}$$

$$-\frac{i\omega}{c^2}\mathbf{E}^{(1,1)}=i\mathbf{k}\times\mathbf{B}^{(1,1)}-\mu_0\sum_j n_{j,0}q_j\mathbf{u}_j^{(1,1)}, \tag{13}$$

where the index $j=1,2$ distinguishes the two particle species (fluids). Assuming a harmonic solution $f\sim\exp[i(kx-\omega t)]$, it is straightforward to derive a dispersion relation (DR) $\omega=\omega(k)$. Without going into details, we note that the DR for perpendicular EM waves in magnetized plasma includes the ordinary (O-) mode dispersion relation

$$\omega^2=\omega_{p,\mathrm{eff}}^2+c^2k^2 \tag{14}$$

(Refs. 13–15) which can easily be shown to satisfy relations (10)–(13); we have defined the effective plasma frequency $\omega_{p,\mathrm{eff}}=(\omega_{p,1}^2+\omega_{p,2}^2)^{1/2}$, where the plasma frequencies $\omega_{p,j}$ were defined above. The DR (14) will be assumed to hold throughout this article. Note, for clarity in notation, that the effective plasma frequency $\omega_{p,\mathrm{eff}}$ reduces to $\omega_p\sqrt{2}$ for pure p.p. (only), where $\omega_{p,1}=\omega_{p,2}=\omega_p$ (since $n_{+,0}=n_{-,0}$; cf. discussion in the previous section), in agreement with previous theoretical results (in fact $\omega_{p,\mathrm{eff}}$ was denoted as ω_p in some previous papers; this trivial notation difference should entail no discrepancy).

The O-mode is associated with a magnetic field (perturbation) which is perpendicular to both $\mathbf{B}_0$ and $\mathbf{k}$, hence $\mathbf{B}^{(1)}=B_y^{(1)}\hat{y}$, and a parallel electric field, i.e. $\mathbf{E}^{(1)}=E_z^{(1)}\hat{z}$; this result, already known from e-i plasmas, is retained in pair plasmas. A set of exact expressions for the first harmonic amplitudes may be obtained in terms of the (reduced) magnetic field (perturbation) amplitude $B_y'=B_y^{(11)}/B_0$. One has

$$u_{\pm,z}^{(11)}=\mp i\frac{\Omega}{k}B_y',\quad E_z'^{(11)}=-\frac{\omega}{ck}B_y',$$

and

$$n_j^{(11)}=u_{j,x}^{(11)}=u_{j,y}^{(11)}=E_x^{(11)}=E_y^{(11)}=0\quad(j=1,2\equiv+,-), \tag{15}$$

where we defined the (common, among pair species) cyclotron frequency $\Omega=ZeB_0/(mc)$ (a positive quantity). The prime in the field components henceforth denotes scaling by B_0 everywhere, i.e., $E'^{(nl)}_{x/y/z}=E^{(nl)}_{x/y/z}/cB_0$, and $B'^{(nl)}_{x/y/z}=B^{(nl)}_{x/y/z}/B_0$.

C. Second order dynamics ($n=2$): Harmonic generation, group velocity

The second-order solution is of the form:

$$\mathbf{S}^{(2)} = \mathbf{S}^{(20)} + [\mathbf{S}^{(21)} \exp i(kx - \omega t) + \text{c.c.}] + [\mathbf{S}^{(22)} \exp 2i(kx - \omega t) + \text{c.c.}]. \quad (16)$$

The exact forms of all harmonic contributions in this expression are explicitly provided in the Appendix.

For $n=2$ and $l=1$, an explicit compatibility condition is obtained in the form:

$$\frac{\partial B_y'}{\partial T_1} + v_g \frac{\partial B_y'}{\partial X_1} = 0. \quad (17)$$

This requirement is satisfied for a wave envelope moving at the group velocity $v_g = \omega'(k) = c^2 k/\omega$. All harmonic amplitudes $S_j^{(11)}$ are therefore functions of $\xi = X_1 - v_g T_1 \equiv \epsilon(x - v_g t)$ (and of $\tau = \epsilon^2 t$, and/or higher orders).

D. Solution up to second order

The solution obtained up to second order in ϵ may be summarized as

$$n_j = n_{j,0} + \epsilon c_j^{(11)} B_y' e^{i\phi} + \epsilon^2 [c_j^{(22)} B_y'^2 e^{i2\phi} + n_j^{(20)}],$$

$$\mathbf{u_j} = \mathbf{0} + \epsilon c_{j,z}^{(11)} B_y' e^{i\phi} \hat{z} + \epsilon^2 \left\{ c_{j,z}^{(21)} \frac{\partial B_y'}{\partial X_1} e^{i\phi} \hat{z} + B_y'^2 e^{i2\phi} [c_{j,x}^{(22)} \hat{x} + c_{j,y}^{(22)} \hat{y}] + \mathbf{u_j}^{(20)} \right\},$$

$$\mathbf{E} = \mathbf{0} + \epsilon c_{el,z}^{(11)} B_y' e^{i\phi} \hat{z} + \epsilon^2 \left\{ c_{el,z}^{(21)} \frac{\partial B_y'}{\partial X_1} e^{i\phi} \hat{z} + B_y'^2 e^{i2\phi} [c_{el,x}^{(22)} \hat{x} + c_{el,y}^{(22)} \hat{y}] + \mathbf{E}^{(20)} \right\},$$

$$\mathbf{B} = B_0 \hat{z} + \epsilon B_y' e^{i\phi} \hat{y} + \epsilon^2 \left[c_{B,y}^{(21)} \frac{\partial B_y'}{\partial X_1} e^{i\phi} \hat{y} + c_{B,z}^{(22)} B_y'^2 e^{i2\phi} \hat{z} + \mathbf{B}^{(20)} \right]$$

for $j = 1, 2 \equiv +, -$; contributions of order $\mathcal{O}(\epsilon^3)$ or higher are omitted everywhere. The exact forms of all coefficients $c_{j,x/y/z}^{(nl)}$ are explicitly provided in the Appendix. Recall that $B_y' = B_y^{(11)}/B_0$ and $\phi = kx - \omega t$. $S_i^{(20)}$ are *arbitrary* state variable corrections satisfying

$$u_{1,x}^{(20)} = -u_{2,x}^{(20)} = cE_y'^{(20)}, \quad u_{1,y}^{(20)} = -u_{2,y}^{(20)} = -cE_x'^{(20)}.$$

We note the generation of secondary harmonics, which is the "signature" of the nonlinear modulation mechanism. See that nonlinearity is essentially generated by the term $u_z^{(11)} B_y^{(11)}$ in the momentum equations, which affects the (coupled, via gyrating motion) perpendicular (to $\mathbf{B}_0$) velocity components, as well as the electric field components in the plane $\perp \mathbf{B}_0$, but—contrary to the first harmonics above—leaves the parallel $\mathbf{E}$ and $\mathbf{u}_j$ components (along $\mathbf{B}_0$) intact. Therefore, the fluid velocities and the electric field possess no second harmonics in the (z) direction parallel to the magnetic field. Quite surprisingly, the component of the electric field in the direction of propagation (along $\hat{x}$) vanishes in pure pair plasmas [cf. expression for $E_x^{(22)}$ in the Appendix].

E. Amplitude evolution equation: $n=3$

Considering the system of equations for $n=3$ and $l=1$, one first needs to ensure that secular terms annihilate, in order for a long-lived analytical solution to exist. This requirement furnishes a compatibility condition to be imposed on the first-harmonic amplitudes, which here takes the form of the nonlinear Schrödinger-type equation (NLSE):

$$i\frac{\partial B_y'}{\partial \tau} + P\frac{\partial^2 B_y'}{\partial \xi^2} + Q|B_y'|^2 B_y' = 0. \quad (18)$$

Recall that the slow time scale is $\tau = \epsilon^2 t$ and the moving envelope space coordinate is $\xi = \epsilon(x - v_g t)$, where the group velocity v_g was defined above. The magnetic field variable is $B_y' = B_y/B_0$. The dispersion coefficient

$$P = \frac{1}{2}\omega''(k) = \frac{c^2 \omega_{p,\text{eff}}^2}{2\omega^3} \quad (19)$$

is related to the curvature of the dispersion relation $\omega(k)$, which is positive (for all wave numbers k). The nonlinearity coefficient Q is related to intrinsic plasma parameters[40] and to the wave frequency ω as

$$Q = Q_A/Q_B, \quad (20)$$

where

$$Q_A = 3\omega_{p,\text{eff}}^2 \Omega^2 [(\Omega^2 - 4\omega^2)\omega_{p,\text{eff}}^2 + 4\omega_{p,1}^2 \omega_{p,2}^2] \quad (21)$$

and

$$Q_B = \omega(c_4 \omega^4 + c_2 \omega^2 + c_0), \quad (22)$$

with

$$c_4 = 48\omega_{p,\text{eff}}^2, \quad c_2 = -4\omega_{p,\text{eff}}^2(3\omega_{p,\text{eff}}^2 + 7\Omega^2), \quad c_0 = \Omega^2[3(\omega_{p,1}^4 + \omega_{p,2}^4) + 10\omega_{p,1}^2 \omega_{p,2}^2 + 4\Omega^2 \omega_{p,\text{eff}}^2]. \quad (23)$$

The expressions for pure pair plasmas are readily obtained by setting $\omega_{p,\text{eff}}^2 = 2\omega_p^2$ everywhere. The dispersion coefficient in the NLSE (18) then simplifies to $P = \omega''(k)/2 = c^2 \omega_p^2/\omega^3$, while the nonlinearity coefficient Q now simply reads

$$Q = \frac{3\Omega^2 \omega_p^2}{2\omega(\Omega^2 - 3\omega^2)}. \quad (24)$$

Note that the sign of P is always positive. However, the sign of Q depends on the relative values of the characteristic frequencies with respect to the EM carrier frequency ω (or wave number k). For ideal pure plasmas, Q is easily seen to be positive (negative) for frequency ω values below (above) a threshold $\Omega/\sqrt{3}$.

IV. MODULATIONAL STABILITY ANALYSIS

The amplitude evolution Eq. (18) is easily seen to support the plane wave solution $\psi = \psi_0 \exp(iQ|\psi_0|^2 \tau)$. The standard linear analysis, which consists of perturbing the amplitude by setting $\hat{\psi} = \hat{\psi}_0 + \epsilon \hat{\psi}_{1,0} \cos(\tilde{k}\xi - \tilde{\omega}\tau)$ (the perturbation wave number $\hat{k}$ and frequency $\hat{\omega}$ should be distinguished

from their carrier wave homolog quantities, denoted by k and ω), leads to the (perturbation) dispersion relation:

$$\tilde{\omega}^2 = P\tilde{k}^2(P\tilde{k}^2 - 2Q|\hat{\psi}_{1,0}|^2). \tag{25}$$

Therefore, if $PQ<0$, the amplitude ψ will be stable to external perturbations. If $PQ>0$, the amplitude ψ is unstable for $\tilde{k}<\sqrt{2Q/P}|\hat{\psi}_{1,0}|$, i.e., for perturbation wavelengths larger than a critical value. This *modulational instability* mechanism is essentially the well-known *Benjamin-Feir* instability, in hydrodynamics, also long-known as an energy localization mechanism in solid state physics and nonlinear optics.[37]

We conclude that the stability profile simply depends of the sign of the product PQ, which may be investigated in terms of the wave number k, in addition to intrinsic plasma parameters.

V. ENVELOPE EXCITATIONS

Summarizing the above analysis, we have obtained a modulated wave here representing the magnetic field correction $\mathbf{B}^{(1)}=B_y^{(1)}\hat{y}$, which is of the form

$$\phi_1^{(1)} = \epsilon\hat{\psi}_0\cos(\mathbf{k}\cdot\mathbf{r} - \omega t + \Theta) + \mathcal{O}(\epsilon^2).$$

The slowly varying amplitude $\psi_0(\xi,\tau)$ (Ref. 41) and phase correction $\Theta(\xi,\tau)$ (both real functions of $\{\xi,\tau\}$; see Ref. 38 for details) are determined by (solving) Eq. (18) for $\psi = \psi_0\exp(i\Theta)$. The different types of solution thus obtained are summarized in the following.

A. Bright-type envelope solitons

We have seen that, for *positive* PQ, the carrier wave is modulationally unstable; it may either collapse, due to (random) external perturbations, or lead to the formation of *bright*-type envelope modulated wave packets, i.e., localized envelope *pulses* confining the fast carrier wave; see Fig. 1. Bright soliton solutions of the NLSE are given by[38]

$$\psi_0 = \left(\frac{2P}{QL^2}\right)^{1/2}\operatorname{sech}\left(\frac{\xi - v_e\tau}{L}\right),$$

$$\Theta = \frac{1}{2P}\left[v_e\xi + \left(\Omega - \frac{v_e^2}{2}\right)\tau\right],$$

where v_e is the envelope velocity; L and Ω represent the pulse's spatial width and oscillation frequency (at rest), respectively. Note that L and ψ_0 satisfy $L\psi_0=(2P/Q)^{1/2}$ =constant (in contrast to KdV solitons, where $L^2\psi_0$=const. instead). Also, the amplitude ψ_0 is independent of the pulse (envelope) velocity v_e here.

B. Dark-type envelope solitons

For $PQ<0$, the carrier wave is modulationally *stable* and may propagate as a *dark* (*black* or *grey*) envelope wave packet, i.e., a propagating localized *hole* (a *void*) amidst a uniform wave energy region. The exact expression for *dark* envelopes reads[38]

$$\psi_0 = \psi_0'\left|\tanh\left(\frac{\xi - v_e\tau}{L'}\right)\right|,$$

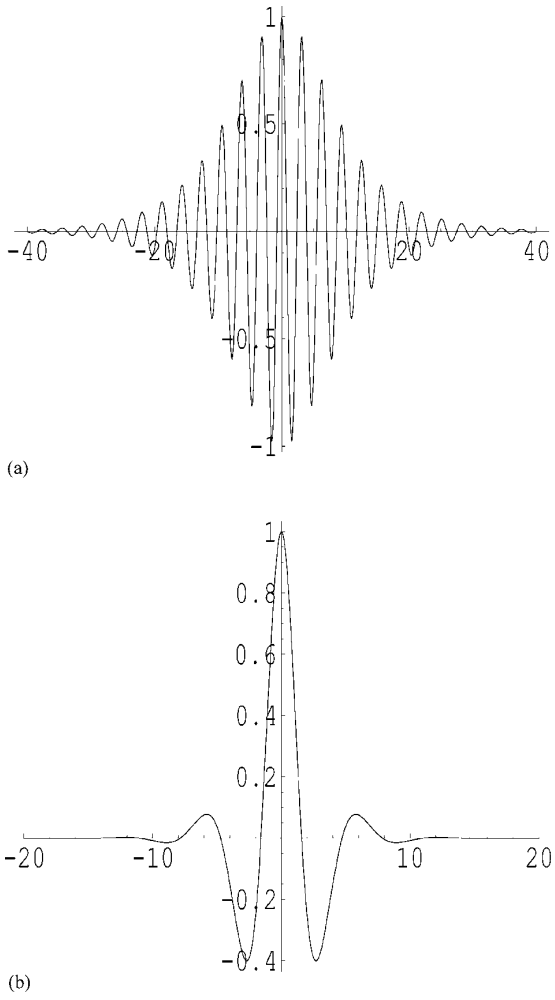

FIG. 1. *Bright* type modulated wave packets (for $PQ>0$), for two different (arbitrary) sets of parameter values.

$$\Theta = \frac{1}{2P}\left[v_e\xi + \left(2PQ\psi_0'^2 - \frac{v_e^2}{2}\right)\tau\right]$$

[see Fig. 2(a)]; again, $L'\psi_0'=(2|P/Q|)^{1/2}$ (=cst.).

The *grey*-type envelope [see Fig. 2(b)], also obtained for $PQ<0$, is given by[38]

$$\psi_0 = \psi_0''\left[1 - d^2\operatorname{sech}^2\left(\frac{\xi - v_e\tau}{L''}\right)\right]^{1/2}$$

and

$$\Theta = \frac{1}{2P}\left[V_0\xi - \left(\frac{1}{2}V_0^2 - 2PQ\psi_0''^2\right)\tau + \Theta_0\right] - S\sin^{-1}\frac{d\tanh\left(\frac{\xi - v_e\tau}{L''}\right)}{\left[1 - d^2\operatorname{sech}^2\left(\frac{\xi - v_e\tau}{L''}\right)\right]^{1/2}}. \tag{28}$$

Here Θ_0 is a constant phase; S denotes the product S $=\operatorname{sign}(P)\times\operatorname{sign}(v_e - V_0)$. The pulse width L''

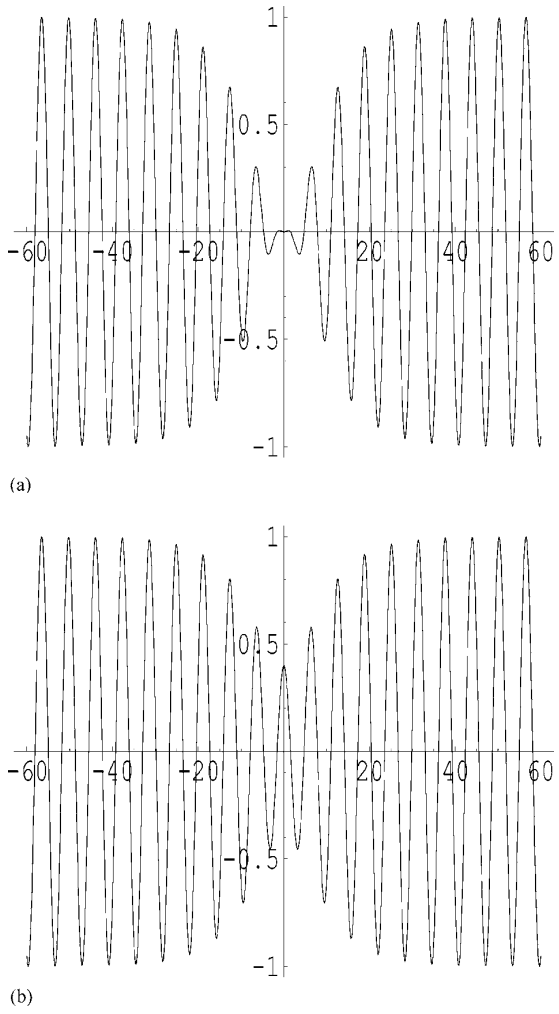

FIG. 2. *Dark*-type modulated wave packets (for $PQ<0$) of the *black* (left) and *grey* (right) kind. See that the amplitude never reaches zero in the latter case.

$=(|P/Q|)^{1/2}/(d\psi_0'')$ now also depends on the real parameter d, given by

$$d^2 = 1 + (v_e - V_0)^2/(2PQ\psi_0''^2) \leq 1.$$

The (real) velocity parameter V_0=const. satisfies[38]

$$V_0 - \sqrt{2|PQ|\psi_0''^2} \leq v_e \leq V_0 + \sqrt{2|PQ|\psi_0''^2}.$$

For $d=1$ (thus $V_0=v_e$), one recovers the *dark* envelope soliton.

VI. MODULATIONAL (IN)STABILITY OF EM WAVES: NUMERICAL ANALYSIS

As was shown above, the (in)stability profile of EM wave packets and the type of envelope excitations propagating in the plasma essentially depend on the coefficient product PQ which, if positive (negative), prescribes instability (stability) and bright (dark, respectively) type envelope solitons. We may now investigate the sign of PQ in various parameter regions.

Since P turns out to be positive, we shall limit ourselves to considering the sign of Q. It is obvious from Eqs. (20)–(23) that the value of Q depends on the plasma frequencies $\omega_{p,1/2}$ (i.e., essentially on the densities $n_{1/2}$), on the cyclotron frequency Ω and on the EM wave frequency ω; recall that the latter is related to the wave number k via the dispersion relation (14).

A. EM wave stability in pure pair plasmas: Stability profile

For "pure" pair plasmas (for $n_3=0$), Eq. (24) suggests that ω_p only affects the value of Q, while Ω determines its sign: $Q>0$ ($Q<0$, respectively) for $\omega<\Omega/\sqrt{3}$ ($\omega>\Omega/\sqrt{3}$). As a first result, in view of the detailed analysis to follow, note that Q is therefore generally negative for cyclotron frequencies Ω lower than $\omega_p\sqrt{6}\approx 2.45\omega_p$ [since $\omega>\omega_p\sqrt{2}\approx 1.414\omega_p$, as prescribed by (14)]; for a low-magnetic-field, therefore, EM waves will always be stable, and will propagate as dark-type envelopes. Note, in passing, that the stability result of Ref. 39 is thus recovered, in the unmagnetized plasma case. For cyclotron frequency values Ω higher than $\omega_p\sqrt{6}\approx 2.45\omega_p$, however, Q changes sign at $\omega=\Omega/\sqrt{3}$, as shown above. This behavior is depicted in Fig. 3, where the ratio Q/P is plotted against ω and Ω (both scaled by ω_p). Recalling that $L\sim|P/Q|^{1/2}\psi_0^{-1}$ determines the width of an envelope soliton (either bright or dark) for a given value of the maximum ψ_0^{-1}, we see that dark excitations will become narrower (higher Q/P) as ω approaches $\Omega/\sqrt{3}$ from below, while bright solitons will be narrower (higher Q/P) as ω approaches $\Omega/\sqrt{3}$ from above.

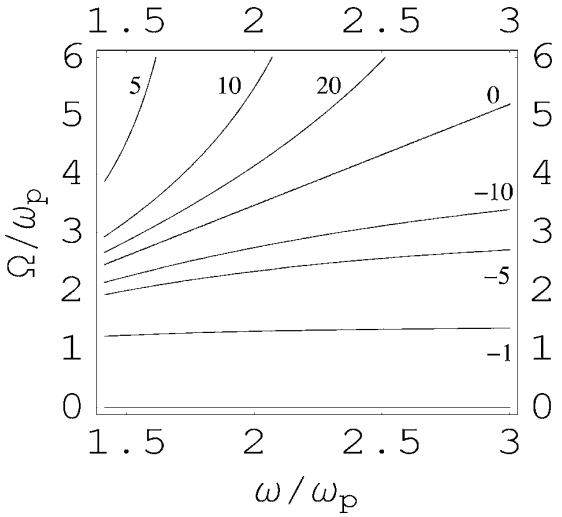

FIG. 3. Coefficient ratio Q/P for "pure" pair plasmas: Contour plot of Q/P values (scaled by ω_p^2/c^2), as provided by Eqs. (19) and (24), vs frequency ω/ω_p (x axis) and cyclotron frequency Ω/ω_p (y axis). The contour values of Q/P are (from top to bottom): 5, 10, 20, 0, −10, −5, −1. The $Q=0$ contour corresponds to $\omega=\Omega/\sqrt{3}$.

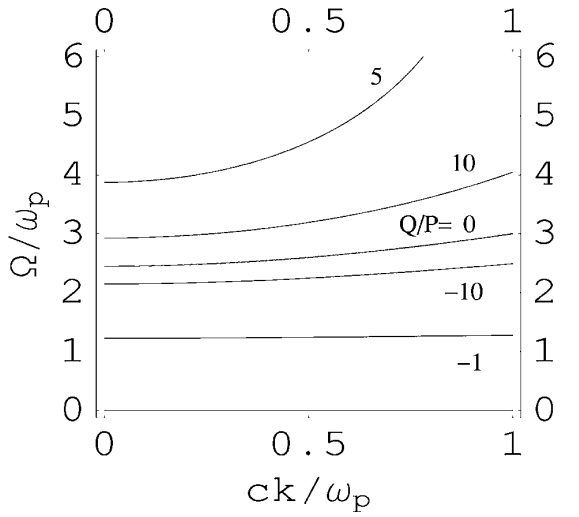

FIG. 4. Coefficient ratio Q/P for "pure" pair plasmas: Contour plot of Q/P values (scaled by ω_p^2/c^2), as provided by Eqs. (19), (24), and (14), vs wave number ck/ω_p (x axis) and cyclotron frequency Ω/ω_p (y axis). The contour values of Q/P are (from top to bottom): 5, 10, 0, −10, −1.

It may be instructive to investigate the stability profile in terms of the wave number k. Combining the dispersion relation (14) with (24), one finds that the coefficient Q changes sign at $k_{cr}=(\Omega^2-6\omega_p^2)^{1/2}/(c\sqrt{3})$, for $\Omega>\omega_p\sqrt{6}$; specifically, $Q<0$ below the threshold k_{cr} (thus prescribing stability and dark-type envelopes), while $Q>0$ for k above k_{cr} (where unstable wave packets may give rise to bright type envelopes). It may be stated, for rigor, that the validity of a fluid model is limited to low wave numbers, say $ck/\omega_p<1$, i.e., for wavelengths $\lambda>\omega_p/c$. For moderately or weakly magnetized plasmas, when $\Omega<\omega_p\sqrt{6}$, Q remains negative, and the wave packets will be stable. This behavior is depicted in Fig. 4, where the ratio Q/P is plotted against wave number k (scaled by ω_p/c) and cyclotron frequency Ω (scaled by ω_p). Again, we see that dark excitations become narrower as k approaches the threshold k_{cr} (where $Q=0$) from below, while bright solitons will be narrower as k approaches k_{cr} from above.

B. Influence of the third species

The effect of the presence of the third background species considered in our model (ions in e-p-i plasmas, "dust" in contaminated pair plasmas) on the stability profile of the EM waves can be traced via the convenient parameter $r=n_{+,0}/n_{-,0}=\omega_{p,+}^2/\omega_{p,-}^2$; recall that r attains values higher (lower) than unity for a negatively (positively) charged third ion species.

We have investigated the dependence of the Q/P ratio on the density misfit (via the parameter r) numerically. It is seen that, for weakly to moderately magnetized plasmas, the ratio Q/P remains negative (for all values of ω and r), suggesting modulational stability and dark-type envelope occurrence. For higher magnetic field values, however, a succession of negative and positive values arises—in the $(k,Q/P)$ or $(\omega,Q/P)$ plane(s), say—which is strongly modified by the values of r. In Fig. 5, we have depicted the ratio Q/P against the cyclotron-to-plasma frequency ratio $\Omega/\omega_{p,1}$, for a fixed value of the frequency ω near the plasma frequency cutoff, i.e. $\omega=\omega_{p,1}\sqrt{2}$. It is seen that for pure pair plasmas [see Fig.

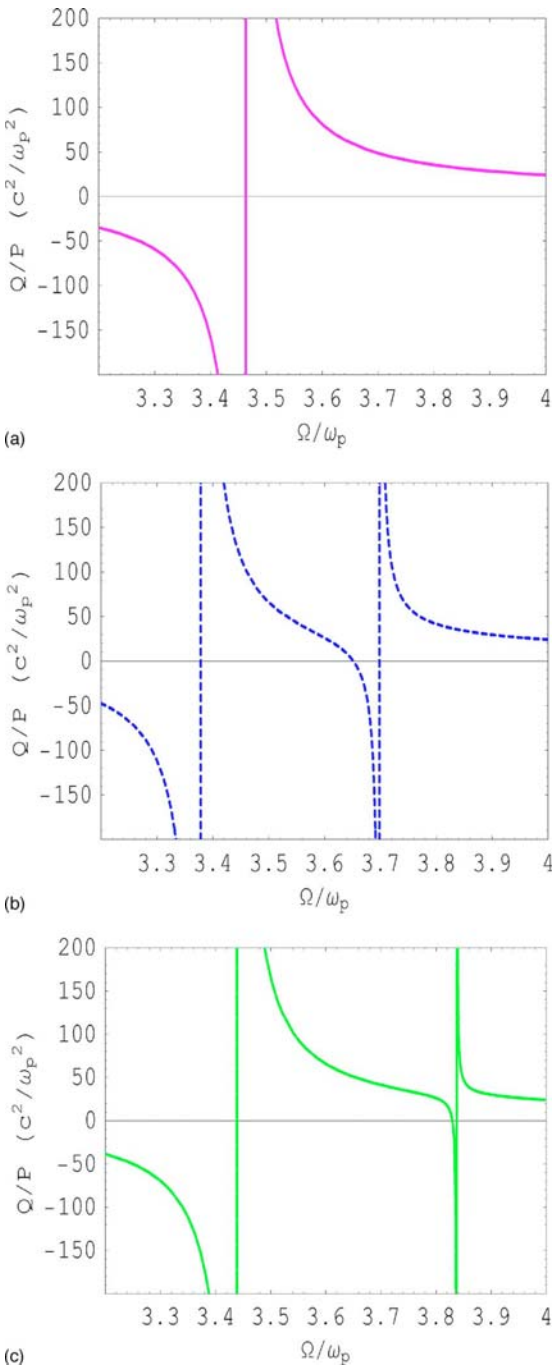

FIG. 5. Coefficient ratio Q/P for: (a) "pure" pair plasmas ($r=1$, i.e., $n_{+,0}=n_{-,0}$); (b) pair plasmas doped with positive background ions ($r=0.5$, i.e. $n_{-,0}=2n_{+,0}$); (c) pair plasmas doped with negative background ions ($r=2$, i.e., $n_{+,0}=2n_{-,0}$). Q/P values (scaled by ω_p^2/c^2), as provided by Eqs. (19), (24), and (14), vs cyclotron frequency Ω/ω_p. Here we have considered a carrier frequency near the plasma frequency cutoff, i.e., $\omega=\omega_{p,1}\sqrt{2}$.

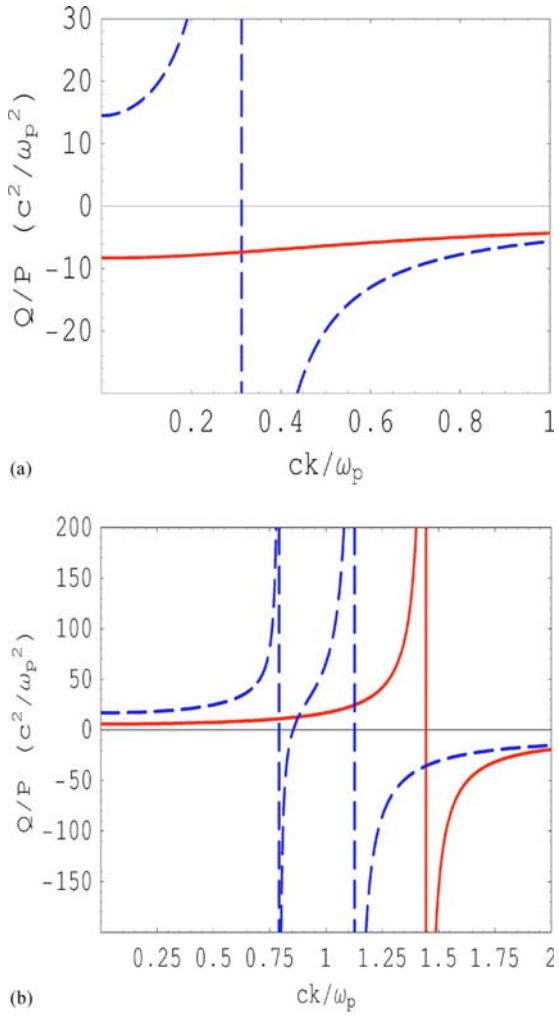

FIG. 6. Coefficient ratio Q/P (scaled by ω_p^2/c^2) vs wave number ck/ω_p, for: (a) $\Omega/\omega_{p,1}=2.1$ and $r=1$ (pure p.p., straight line) or $r=2$ (negative third ion species, dashed curve); (b) $\Omega/\omega_{p,1}=3.5$ and $r=1$ (pure p.p., straight line) or $r=0.5$ (positive third ion species, dashed curve).

5(a)], a qualitative transition occurs near $\Omega \approx 3.455\omega_{p,1}$, above (below) which value EM waves will be unstable (stable), and only bright (dark, respectively) type envelopes may occur. For pair plasmas "contaminated" with a negative third ion species [see Fig. 5(b)], though, we witness the appearance of one more pole [for $\Omega \approx 3.7\omega_{p,1}$, say, in Fig. 5(b)], slightly below which one more modulational stability region occurs. Therefore, the inclusion of an extra third ion species in p.p. tends to stabilize the wave envelope, for high magnetic field values, and also affects the characteristics of envelope structures: width, form, stability. A similar behavior is observed in Fig. 5(c), where we have considered a positive third ion species (e.g., ions, in e-p-i plasma).

In Fig. 6, we have depicted the ratio Q/P against the wave number k, for a fixed value of the cyclotron-to-plasma frequency ratio $\Omega/\omega_{p,1}$. The conclusions drawn from these plots are similar to the above: the addition of an extra third species seems able to destabilize the wave envelope and/or modify the localized envelope characteristics.

VII. SUMMARY AND CONCLUSIONS

Summarizing our results, we have considered the propagation of nonlinear amplitude-modulated EM wave packets in a pair plasma, consisting of two pair ion species (negative-positive), possibly in addition to an extra (third) massive ion species in the background. We have thus aimed at modeling pair-plasmas (as formed in recent fullerene experiments), either "pure" or contaminated by charged massive defects (viz., dust), in addition to electron-positron and electron-positron-ion plasmas (neglecting annihilation effects). The carrier wave was assumed to obey the dispersion characteristics of the ordinary (O-) mode, propagating in a direction perpendicular to the ambient magnetic field. By adopting a reductive-perturbation (multiple scales) technique, we have shown that the magnetic field perturbation bears the form of a nonlinearly modulated wave packet, whose envelope is governed by a nonlinear Schrödinger-type equation. The investigation of the modulational stability of the envelope against perturbations has pointed out the existence of a rich profile, in terms of the interplay between relevant plasma parameters, e.g., the plasma frequency (-ies) $\omega_{p,1/2}$, the cyclotron frequency Ω, and the carrier wave frequency ω. In particular, electromagnetic wave packets were shown to exist, either in the form of an envelope pulse (bright envelope soliton), or a void (dark envelope soliton, a hole), depending on the plasma parameters. The presence of the background ion species was shown to modify the characteristics of these excitations, and/or affect the stability profile of the modulated wave packets.

These results are in relevance with plasma observations, in both experimental and astrophysical environments, e.g., related to signal detection from pulsars, where e-p plasmas are believed to exist, or laboratory experiments involving pair (fullerene) ion creation under controlled conditions. Our theoretical predictions may be tested, and will hopefully be confirmed, by appropriate experiments of that kind.

ACKNOWLEDGMENTS

The authors express their appreciation and gratitude for a number of long inspiring discussions with G. S. Lakhina (Indian Institute of Geomagnetism, Bombay, India), M. Hellberg (University of KwaZulu-Natal, South Africa), and T. Cattaert (University of Gent, Belgium). I.K. and N.C. acknowledge the hospitality of Sterrenkundig Observatorium, University of Gent (Belgium), where this work was mainly carried out.

Funding from the FWO (Fonds Wetenschappelijk Onderzoek-Vlaanderen, Flemish Research Fund) during the course of this work is gratefully acknowledged. I.K. acknowledges support from the Deutsche Forschungsgemeinschaft (DFG) under the Emmy-Noether program (Grant No. SH 93/3-1), during the last part of this work.

APPENDIX: SECOND ORDER HARMONIC AMPLITUDES: $n=2$, $l=0,1,2$

The first harmonic amplitudes ($n=2$, $l=1$) are given by

$$u_{j,z}^{(21)} = (-1)^j \frac{c^2\omega_{p,\mathrm{eff}}^2\Omega}{\omega^2 k^2}\frac{\partial B_y'}{\partial X_1},$$

$$E_z^{(21)} = i\frac{\omega}{ck^2}\frac{\partial B_y'}{\partial X_1}, \tag{A1}$$

$$B_y^{(21)} = -i\frac{\omega^2+\omega_{p,\mathrm{eff}}^2}{\omega^2 k}\frac{\partial B_y'}{\partial X_1},$$

while all remaining coordinates vanish, i.e.,

$$n_j^{(21)} = u_{j,x/y}^{(21)} = E_{x/y}^{(21)} = B_{x/z}^{(21)} = 0.$$

The second harmonic amplitudes ($n=2$, $l=2$) are given by

$$u_{j,x}^{(22)} = \frac{\omega n_j^{(22)}}{k n_{j,0}} = \frac{D_{j,x}^{(22)}}{D_0^{(22)}}B_y'^2,$$

$$u_{j,y}^{(22)} = \frac{D_{j,y}^{(22)}}{D_0^{(22)}}B_y'^2, \quad u_{j,z}^{(22)} = 0,$$

$$E_x^{(22)} = \frac{D_{el,x}^{(22)}}{D_0^{(22)}}B_y'^2, \tag{A2}$$

$$E_y^{(22)} = \frac{\omega}{ck}B_z^{(22)} = \frac{D_{el,y}^{(22)}}{D_0^{(22)}}B_y'^2, \quad E_z^{(22)} = B_y^{(22)} = 0$$

(for $j=1,2$) where

$$D_{1,x}^{(22)} = 6c^2 k\omega\Omega^2\omega_{p,\mathrm{eff}}^2(4\omega^2-\Omega^2-2\omega_{p,2}^2),$$

$$D_{2,x}^{(22)} = 6c^2 k\omega\Omega^2\omega_{p,\mathrm{eff}}^2(4\omega^2-\Omega^2-2\omega_{p,1}^2),$$

$$D_{1,y}^{(22)} = ic^2 k\Omega^3\{-4\omega_{p,\mathrm{eff}}^2(4\omega^2-\Omega^2) - 2\omega_{p,2}^2(4c^2k^2-4\omega^2-\omega_{p,1}^2) - 2\omega_{p,2}^4\},$$

$$D_{2,y}^{(22)} = -ic^2 k\Omega^3\{-4\omega_{p,\mathrm{eff}}^2(4\omega^2-\Omega^2) - 2\omega_{p,1}^2(4c^2k^2-4\omega^2-\omega_{p,2}^2) - 2\omega_{p,1}^4\},$$

$$D_{\mathrm{el},x}^{(22)} = -3ick\omega_{p,\mathrm{eff}}^2\Omega(4\omega^2-\Omega^2)(\omega_{p,1}^2-\omega_{p,2}^2),$$

$$D_{\mathrm{el},y}^{(22)} = 2ck\omega\Omega^2[(\Omega^2-4\omega^2)\omega_{p,\mathrm{eff}}^2+4\omega_{p,1}^2\omega_{p,2}^2],$$

and

$$D_0^{(22)} = c^2k^2\{-64\omega^6+32(2\omega^2-\omega_{p,\mathrm{eff}}^2+\Omega^2)\omega^4 - 4[4c^2k^2(2\Omega^2+\omega_{p,\mathrm{eff}}^2)+\Omega^4+\omega_{p,\mathrm{eff}}^4 + 2\Omega^2\omega_{p,\mathrm{eff}}^2]\omega^2 - \Omega(\omega_{p,1}^2-\omega_{p,2}^2)^2 + 4c^2k^2\Omega^2(\omega_{p,\mathrm{eff}}^2+\Omega^2)\}. \tag{A3}$$

A zeroth harmonic (constant, nonoscillating) contribution ($n=2$, $l=0$) is also found to second order. The perpendicular velocity and field amplitudes satisfy

$$u_{1,x}^{(20)} = -u_{2,x}^{(20)} = cE_y'^{(20)},$$

$$u_{1,y}^{(20)} = -u_{2,y}^{(20)} = -cE_x'^{(20)}, \tag{A4}$$

while all remaining variables are left arbitrary.

[1] V. L. Ginzburg, Sov. Phys. Usp. **14**, 83 (1971); P. A. Sturrock, Astrophys. J. **164**, 529 (1971).
[2] M. A. Ruderman and P. G. Sutherland, Astrophys. J. **196**, 51 (1975).
[3] R. N. Manchester and J. H. Taylor, *Pulsars* (Freeman, San Francisco, 1977).
[4] F. C. Michel, Rev. Mod. Phys. **54**, 1 (1982).
[5] F. C. Michel, *Theory of Neutron Star Magnetospheres* (University of Chicago Press, Chicago, 1991); see also various articles in *Pulsars: Problems and Progress*, edited by S. Johnston, M. A. Walker, and M. Bailes, Astrophysical Society (ASP) of the Pacific Conference Series 105 (ASP, San Francisco, 1996).
[6] H. R. Miller and P. J. Witta, *Active Galactic Nuclei* (Springer-Verlag, Berlin, 1987), p. 202; M. C. Begelman, R. D. Blandford, and M. D. Rees, Rev. Mod. Phys. **56**, 255 (1984).
[7] M. L. Burns, *Positron-Electron Pairs in Astrophysics*, edited by M. L. Burns, A. K. Harding, and R. Ramaty (American Institute of Physics, New York, 1983), p. 281.
[8] G. W. Gibbons, S. W. Hawking, and S. Siklos, *The Very Early Universe* (Cambridge University Press, Cambridge, 1983).
[9] E. P. Liang, S. C. Wilks, and M. Tabak, Phys. Rev. Lett. **81**, 4887 (1998); C. Gahn, G. D. Tsakiris, G. Pretzler *et al.*, Appl. Phys. Lett. **77**, 2662 (2000).
[10] R. G. Greaves, M. D. Tinkle, and C. M. Surko, Phys. Plasmas **1**, 1439 (1994); J. Zhao, J. I. Sakai, and K. Nishikawa, *ibid.* **3**, 844 (1996); R. G. Greaves and C. M. Surko, Phys. Rev. Lett. **75**, 3846 (1995).
[11] P. Helander and D. J. Ward, Phys. Rev. Lett. **90**, 135004 (2003).
[12] W. Oohara and R. Hatakeyama, Phys. Rev. Lett. **91**, 205005 (2003); **95**, 175003 (2005).
[13] N. A. Krall and A. W. Trivelpiece, *Principles of Plasma Physics* (McGraw-Hill, New York, 1973), p. 9.
[14] D. G. Swanson, *Plasma Waves* (Institute of Physics, Bristol, 2003), p. 19.
[15] Th. Stix, *Waves in Plasmas* (American Institute of Physics, New York, 1992), pp. 6 and 26.
[16] N. Iwamoto, Phys. Rev. E **47**, 604 (1993).
[17] G. A. Stewart and E. W. Laing, J. Plasma Phys. **47**, 295 (1992).
[18] G. P. Zank and R. G. Greaves, Phys. Rev. E **51**, 6079 (1995).
[19] V. Tsytovich and C. B. Wharton, Comments Plasma Phys. Controlled Fusion **4**, 91 (1978).
[20] J. Vranjes and S. Poedts, Plasma Sources Sci. Technol. **14**, 485 (2005).
[21] F. Verheest and T. Cattaert, Phys. Plasmas **11**, 3078 (2004).
[22] F. Verheest and T. Cattaert, Phys. Plasmas **12**, 032304 (2005).
[23] F. Verheest, T. Cattaert, G. S. Lakhina, and S. V. Singh, J. Plasma Phys. **70**, 237 (2004).
[24] H. Hasegawa and Y. Ohsawa, J. Phys. Soc. Jpn. **73**, 1764 (2004).
[25] I. Kourakis, A. Esfandyari-Kalejahi, M. Mehdipoor, and P. K. Shukla, Phys. Plasmas **13**, 052117 (2006).
[26] M. Salahuddin, H. Saleem, and M. Saddiq, Phys. Rev. E **66**, 036407 (2002).
[27] A. Esfandyari-Kalejahi, I. Kourakis, M. Mehdipoor, and P. K. Shukla, J. Phys. A **39**, 13817 (2006).
[28] A. Esfandyari-Kalejahi, I. Kourakis, and P. K. Shukla, Phys. Plasmas **13**, 122310 (2006).
[29] J. Sakai and T. Kawata, J. Phys. Soc. Jpn. **49**, 753 (1980).
[30] F. Verheest, Phys. Lett. A **213**, 177 (1996).
[31] J. Zhao, K. Nishikawa, and J. I. Sakai, Phys. Plasmas **1**, 103 (1994).
[32] T. Cattaert, I. Kourakis, and P. K. Shukla, Phys. Plasmas **12**, 012319 (2005).
[33] S. Irie and Y. Ohsawa, J. Phys. Soc. Jpn. **70**, 1585 (2001).
[34] N. Cramer, Proceedings of the EPS 33, Rome, 2006, paper No. D2.001.
[35] T. Taniuti and N. Yajima, J. Math. Phys. **10**, 1369 (1969); N. Asano, T. Taniuti, and N. Yajima, *ibid.* **10**, 2020 (1969).
[36] A. Hasegawa, Phys. Rev. A **1**, 1746 (1970); Phys. Fluids **15**, 870 (1972).
[37] A. Hasegawa, *Plasma Instabilities and Nonlinear Effects* (Springer-Verlag, Berlin, 1975).
[38] R. Fedele and H. Schamel, Eur. Phys. J. B **27**, 313 (2002).

[39] G. S. Lakhina and B. Buti, Astrophys. Space Sci. **79**, 25 (1981).

[40] It may be noted, for the sake of rigor, that a secondary contribution δQ to the nonlinearity coefficient (viz. $Q \to Q + \delta Q$) also results from the algebra; it is associated with the (arbitrary) constant density perturbations, $n_1^{(20)}$ and $n_2^{(20)}$ as $\delta Q = -(\omega_{p,1}^2 n_1^{(20)}/n_{1,0} + \omega_{p,2}^2 n_2^{(20)}/n_{2,0}^2)/(2\omega)$. δQ was assumed to vanish here, by assuming a quiescent (zero overall motion) plasma.

[41] In fact, the amplitude here is $\hat{\psi}_0 = 2\psi_0$; cf. Euler's formula: $e^{ix} + e^{-ix} = 2\cos x$ $(x \in \Re)$.